https://doi.org/10.5194/egusphere-2026-4354
Preprint. Discussion started: 28 July 2026

Climate Variability, Grain Supply, and Food Security in Ancient Rome

Devi Taelman[1], Luigi Oddo[1], Duncan Keenan-Jones[2], Danielle Verdon-Kidd[3], Paul Erdkamp[1]

[1]Research Group Transdisciplinary Agrifood Studies (TAFS), Vrije Universiteit Brussel, Brussels, 1050, Belgium
[2]Department of Classics, Ancient History, Archaeology, and Egyptology, The University of Manchester, Manchester, M13 9PL, United Kingdom
[3]School of Science, The University of Newcastle, Callaghan, NSW 2308, Australia

Correspondence to: Devi Taelman (devi.taelman@vub.be)

Abstract. The Roman world has become a central case in debates on past climate–society interactions, particularly regarding the empire's expansion, transformation, and decline. However, despite growing recognition that these interactions were mediated through complex socio-economic and ecological processes, the mechanisms through which climatic variability translates into historical outcomes are rarely investigated explicitly. In this paper, we investigate whether climatic variability was systematically associated with historically attested food shortages in ancient Rome, explicitly accounting for changes in the geographical configuration of the city's provisioning system. Combining annual palaeoclimatic reconstructions from climate field reconstructions (PHYDA and GEDA) with a dataset of 55 attested shortage events for the period 1–650 CE, we analyse temperature and hydroclimatic variability across Rome's principal grain-supplying regions. The analysis combines probit regression models with Monte Carlo simulations to test associations with both short-term climatic shocks and sustained climatic anomalies. The results provide no evidence for a sfigu, system-wide climate–shortage relationship. Throughout the Imperial and Late Antique periods, statistical associations are weak and regionally variable, suggesting a provisioning system that buffered regional climatic variability. A clearer, albeit modest, climatic signal emerges only after the contraction of Rome's supply network in the late fifth century CE. Overall, the findings indicate that, based on historically attested food shortages, climatic variability influenced Rome's food security not as a direct or uniform trigger, but as a conditional stressor whose effects depended on the changing structure of Rome's provisioning system.

1 Introduction

Climate change and its impact on global society rank among the most urgent and politically charged challenges of our time. Contemporary debates over its causes and long-term effects on present-day society inevitably shape how scholars interpret past climate variability and its role in societal change, thereby contributing to simplistic cause-and-effect readings that frame complex historical transformations primarily in environmental terms. The Roman world has become a prominent case in narratives of climate–society dynamics, particularly in relation to the empire's expansion, transformation, and decline (cf. Marx et al., 2018). While such studies have drawn attention to possible links between extreme or prolonged climatic

https://doi.org/10.5194/egusphere-2026-4354
Preprint. Discussion started: 28 July 2026

variability and episodes of political, economic, and demographic disruption, establishing robust mechanisms that connect climatic anomalies to specific historical outcomes remains methodologically challenging. A growing body of recent scholarship (e.g., Bernard et al., 2023; Degroot et al., 2021; Erdkamp, 2021; Haldon et al., 2018) highlights the need to move beyond broad correlations, deterministic reasoning, and large-scale climatic labels (such as the so-called Roman Climatic Optimum and Late Antique Little Ice Age) and instead account for the historically specific mechanisms and processes through which climatic variability was translated into social outcomes. The impact of climate variability on pre-industrial societies was rarely direct or linear. Rather, environmental pressures were filtered through complex socio-economic and ecological mechanisms, with agriculture forming a key interface between climatic conditions and societal response (Daems et al., 2024; Degroot et al., 2021, 2022; Deij et al., 2026; Slavin, 2016; Van Bavel et al., 2019; White et al., 2023).

This paper addresses these issues by focusing on the city of Rome in the Imperial, Late Antique, and Early Medieval periods, for which food shortages are relatively well attested in ancient sources. The objective of this paper is to examine if climatic variability increased the likelihood of food stress in ancient Rome, taking into account the city's agrarian and provisioning structures. More specifically, it tests whether, and under what historically specific conditions, climatic variability interacted with agrarian and institutional constraints to shape the likelihood of food stress. To this end, we (1) recognise and account for the regional variability of the palaeoclimatic record, and (2) focus explicitly on agricultural output and the resultant food supply as the principal mediators through which climate influenced societal dynamics. By statistically analysing the relationship between historically attested food shortages and high-resolution palaeoclimatic evidence, we evaluate how climatic conditions interacted with agricultural production and provisioning structures to shape the probability of food shortages in Rome. In doing so, we account for the evolving nature of the city's food supply system, particularly the shifting balance and interaction between local production as well as regional and long-distance imports.

2 Rome's Grain Supply and Agroclimatic Context

As Rome expanded from a regional centre in the Republican period to a metropolis of nearly one million inhabitants by the Early Empire (Morley, 1996) and an estimated annual grain requirement surpassing 150,000 tonnes (Erdkamp, 2013; Rickman, 1980), securing a stable food supply became a major logistical challenge for its authorities. Initially supplied by its immediate hinterland, Rome began to rely increasingly on imports from Sicily and Sardinia to meet its growing demand for grain after the Second Punic War (Erdkamp, 2000, 2005). This growing dependence on external supplies transformed the city's food supply and distribution into a matter of public administration and political negotiation. This transformation found formal expression in 123 BCE through Gaius Gracchus' *lex frumentaria*, which instituted regular distributions of subsidised grain (*frumentationes*, the so-called "grain dole") and established Rome's first public granaries (Erdkamp, 2005; Geraci, 2018). In the same period, the fertile zones of Africa Proconsularis (notably Byzacena and the Bagradas/Medjerda valley) emerged as major suppliers alongside the city's hinterland, Sicily, and Sardinia. Following the annexation of Egypt in 31–30

https://doi.org/10.5194/egusphere-2026-4354
Preprint. Discussion started: 28 July 2026

BCE, the African provinces and Egypt became the cornerstones of Rome's provisioning (Erdkamp, 2005; Geraci, 2018; Rickman, 1980). Even though the relative importance of Sicily, Sardinia, and Rome's hinterland declined, their geographic proximity continued to provide a strategic buffer against disruptions in overseas grain shipments from North Africa and Egypt, particularly at the start of the sailing season when imports could be disrupted even without harvest failure. By this stage, and continuing into Late Antiquity, Rome's provisioning system, known as the *annona*, relied heavily on publicly organised supply mechanisms. Grain was obtained through a combination of taxation-in-kind, shares of the harvest, and rents from imperial estates (e.g., Africa Proconsularis, Sicily, and Sardinia), as well as, in the case of Egypt, through a more structured fiscal regime of fixed land tax. It was then distributed freely or at subsidised prices to the inhabitants of Rome, with private trade playing only a minor role within this essentially state-controlled system (Erdkamp, 2005). After the foundation of Constantinople in 330 CE, Egypt's grain was redirected to the new capital, leaving Africa Proconsularis, Sicily, Sardinia, and the Roman hinterland as the city's primary suppliers until the mid-fifth century. Following the Vandal conquest of North Africa, Rome, though severely diminished in population, relied increasingly on supplies from the Italian Peninsula, Sicily, and Sardinia for its provisioning (Linn, 2012; Wijnendaele, 2019).

This implies that Rome's food supply system functioned across multiple ecological zones, each defined by its own climatic and agricultural regime. In the Italian Peninsula, Sicily, Sardinia, and Africa, agriculture was predominantly rain-fed (Heinrich and Hansen, 2021; Taelman et al., in press). Cereals were typically sown in autumn and harvested in late spring or early summer to avoid the peak heat of July and August. Summer conditions, however, could affect yields in distinct ways: for example, drought during late growth stages reduced grain filling, whereas excessive rainfall at harvest could delay cutting and increase susceptibility to fungal diseases (Heinrich and Hansen, 2021). Only minor crops such as millets were sown in summer as drought-tolerant supplements rather than primary staples (Heinrich and Hansen, 2021; Heinrich, 2017). At higher elevations, where cooler and wetter conditions limited autumn sowing, crops could be planted in early spring using varieties capable of tolerating the summer heat during maturation (Columella, *De Re Rustica* 2.9.3, 16, Pliny the Elder, *Nat. Hist*, 18.69-70, *CIL* VI.2305 = ILS 8745). In contrast to these rain-fed Mediterranean regimes, Egyptian agriculture depended on the climate-driven annual inundation of the Nile, whose flood-height variability determined both the extent of cultivable land and the deposition of fertile silt. Insufficient floods reduced the area available for sowing and limited soil renewal, thereby constraining yields, whereas excessively high floods could damage dikes and irrigation infrastructure, delay planting, disrupt the agricultural calendar, or leave fields waterlogged (Huebner, in press).

3 Data and Methods

3.1 Historical Evidence for Food Shortages in Ancient Rome

A dataset of historical attestations on food shortages and famines (*fames* in Latin) in ancient Rome, covering 500 BCE to 650 CE, was compiled from the modern syntheses of Garnsey (1988) and Stathakopoulos (2004), which in turn draw on

https://doi.org/10.5194/egusphere-2026-4354
Preprint. Discussion started: 28 July 2026

ancient textual and numismatic evidence. Their compilations were supplemented by one additional event, recorded in the *Liber Pontificalis* for 531 CE. All recorded entries concern shortages of basic food supplies. Milder shortages typically reflect short-term disruptions, "*indicated by rising prices, popular discontent, [and] hunger*", while catastrophic famines are those that "*lead to starvation*" (Garnsey, 1988). To ensure analytical consistency, only events with secure chronological anchoring, reasonable historical evidence, and explicit relevance to the city of Rome were retained.

The resulting dataset for the period from 500 BCE to 650 CE consists of 104 events (Table S1), including both acute crises and longer periods of food stress. In cases where multiple consecutive years were affected, each year was counted as a separate entry. On average, this corresponds to one attested shortage approximately every 11 years. Notable clusters of reported events occur in the fifth century BCE, the late first century BCE to early first century CE, around 400 CE, and in the sixth century CE, while multi-decade gaps are evident particularly in the fourth and third centuries BCE (when the full text of Livy's Republican History is lost), and the third century CE (Fig. 1). These concentrations and lacunae should, however, be interpreted with caution, as they may reflect not only genuine fluctuations in the occurrence of food crises, but also changes in the nature, survival, and narrative priorities of historical writing (for example, shifts in genre conventions, authorial agendas, and recording practices; cf. Erdkamp, 2000, 2019; Van Bavel et al., 2019). The dataset should therefore be understood as a source-limited sample rather than a comprehensive catalogue of all historical shortages, that is, as a conservative estimate of the food shortage frequency that provides an event framework against which environmental variability can be evaluated. Accordingly, the analyses presented below do not seek to reconstruct the full occurrence of food shortages in ancient Rome, but rather to evaluate whether food shortages preserved in the surviving textual tradition are associated with unusual climatic conditions.

The temporal scope of the study is further restricted to the period between 1 CE and 650 CE for three reasons: (1) the historiographical unreliability of Early and Mid-Republican food shortage accounts, which are largely based on later historical sources and tend to reflect the political ideologies and narrative frameworks of the Late Republic and early Empire, rather than contemporaneous documentation (Erdkamp, 2000); (2) the inclusion of the transitional early medieval centuries during which Rome's grain redistribution system dissolved and the Mediterranean political economy was reconfigured (Sect. 2), and the latest horizon for which food shortage attestations remain sufficiently regular and contextually secure to permit systematic comparison; and (3) the availability of high-resolution annual palaeoclimatic data only for the Common Era (Sect. 3.2). Of the 104 historically attested shortage years, 55 fall within the 1–650 CE interval considered for statistical analysis (Sect. 3.3).

https://doi.org/10.5194/egusphere-2026-4354
Preprint. Discussion started: 28 July 2026

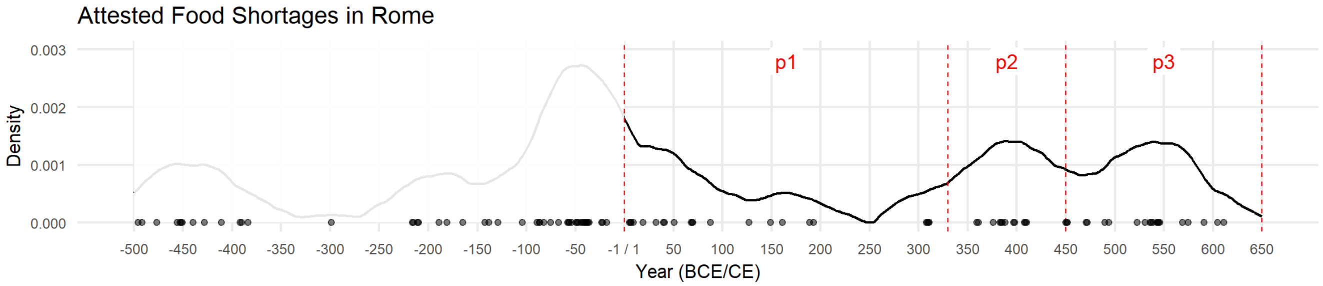

Figure 1. Attested food shortages in Rome (500 BCE to 650 CE). Black points represent years in which historical sources record a food shortage (n = 104). The black curve represents the probability density of these events, estimated using a kernel density approach (Epanechnikov kernel, 25-year bandwidth). The dashed lines indicate the boundaries of the distinct phases in Rome's food supply system (Sect. 3.3). The BCE period (greyed area) is not included in the analysis, as it cannot be directly compared with palaeoclimatic data due to data limitations.

3.2 Palaeoclimate Reconstruction Data

To assess climatic variability at the temporal scale relevant to Rome's food supply system, we employ gridded palaeoclimate reconstructions, known as climate field reconstructions (CFRs). By synthesising information from multiple proxy records within a coherent spatio-temporal framework, CFRs generate spatially continuous palaeoclimatic reconstructions and enable systematic comparison, which cannot be achieved using site-specific proxy records (Amrhein et al., 2020; Tierney et al., 2025). Because Rome's grain supply extended across multiple ecological regions, such regionally resolved reconstructions allow climatic variability to be examined at the interregional scale on which the provisioning system functioned. While CFRs smooth local variability and inherit uncertainties related to proxy availability, proxy system characteristics, and model structure (cf. Amrhein et al., 2020; Anchukaitis and Smerdon, 2022; Smerdon et al., 2023; Tierney et al., 2025), they capture large-scale patterns that are central to the present analysis.

In this study, we draw on two CFR datasets. Annual summer (June–August; JJA) temperature data were obtained from the Paleo Hydrodynamics Data Assimilation (PHYDA) (Steiger et al., 2018) and converted to anomalies relative to the 1961–1990 mean (hereafter TA: Temperature Anomalies).[1] Annual hydroclimatic data were derived from the Great Eurasian Drought Atlas (GEDA) and expressed as JJA scPDSI (self-calibrated Palmer Drought Severity Index) (Cook et al., 2024).[2] The scPDSI is a widely used drought metric that integrates temperature, precipitation, and a soil-moisture balance model to

[1] PHYDA combines 2,978 palaeoclimatic proxy time series (including tree rings, lake sediments, speleothems and ice cores) within the constraints of a global atmosphere-ocean climate model using a data assimilation approach. The reconstruction is based on a 998-member climate-model ensemble, from which posterior ensemble estimates and associated uncertainty statistics are derived. It provides temperature data at annual and seasonal (June–August and December–February) scales for the Common Era, at a spatial resolution of 2° (lat) x 2° (lon) (Steiger et al., 2018).
[2] GEDA is tree-ring-based reconstruction of scPDSI, based on 1,021 records. The reconstruction is derived from a 9-member ensemble of optimised reconstructions, from which the ensemble-mean was used to produce the final dataset. It provides summer (June–August) scPDSI data across Eurasia and sub-Saharan Africa for the Common Era, at a spatial resolution of 0.5° (lat) x 0.5° (lon) (Cook et al., 2024).

quantify relative wetness and dryness, with negative values indicating drier-than-average and positive values wetter-than-average conditions. Its self-calibrated formulation improves spatial comparability by adjusting the index to local climate regimes (Wells et al., 2004). For each of ancient Rome's main food provisioning regions, JJA TA and scPDSI time series (Tables S2 and S3), representing the final growing and harvesting stages of Mediterranean cereal agriculture (Sect. 2), were calculated by averaging PHYDA (TA) and GEDA (scPDSI) grid cell values falling within the geographic bounding boxes defined in Table 1. For Egypt, the timeseries of scPDSI (Table S3) were extracted from GEDA for the grid cells covering the Ethiopian Highlands (encompassing the Blue Nile, Atbara, and Baro-Akobo river basins), where inter-annual variability in summer monsoon rainfall, responsible for approximately 85 % of the Nile's annual discharge (Eldardiry and Hossain, 2019; Yitayew and Melesse, 2011), controlled flood magnitude and thus the extent of cultivable land along the Egyptian Nile Valley (Sect. 2). All analyses reported in this study use the ensemble mean reconstructions for TA (PHYDA) and scPDSI (GEDA). To account for the uncertainty inherent in palaeoclimatic reconstructions, the sensitivity of the results to uncertainty in CFR production was evaluated for TA (PHYDA) using the 5th and 95th percentile ensemble reconstructions, as described in Sect. 3.3.

Table 1. Geographic bounding boxes used to extract palaeoclimate data (PHYDA temperature anomalies and GEDA scPDSI values) for the main food provisioning regions of ancient Rome.

Region	Latitude	Longitude
Hinterland of Rome (ROM)	41.43° N – 42.34° N	11.88° E – 13.10° E
Sicily (SIC)	36.58° N – 38.54° N	12.35° E – 15.62° E
Sardinia (SAR)	38.70° N – 41.24° N	7.96° E – 9.97° E
Africa Proconsularis (AFR)	33.74° N – 37.47° N	6.23° E – 11.18° E
Nile Sources / Ethiopian Highlands (Egypt) (NIL)	9.13° N – 13.55° N	33.84° E – 38.16° E

At a multi-decadal scale, as illustrated by the 50 year lowpass filtered TA values (Fig. 2), temperature variability is broadly synchronous across the study regions. Differences lie mainly in anomaly magnitude, with values ranging from approximately -0.75 °C to +0.75 °C. Reconstructions indicate modest to high positive anomalies during the period 1–150 CE, a return to average or slightly cooler conditions between 150 and 190 CE, and a third century marked by warmer conditions and higher-frequency variability with oscillations in the order of about 25 years. Relatively stable, near-average conditions characterise most of the fourth and fifth centuries, followed by a brief warming at the start of the sixth century and a pronounced cool interval centred in the middle of the sixth century. From the seventh century onwards, near-average conditions can be observed.

https://doi.org/10.5194/egusphere-2026-4354
Preprint. Discussion started: 28 July 2026

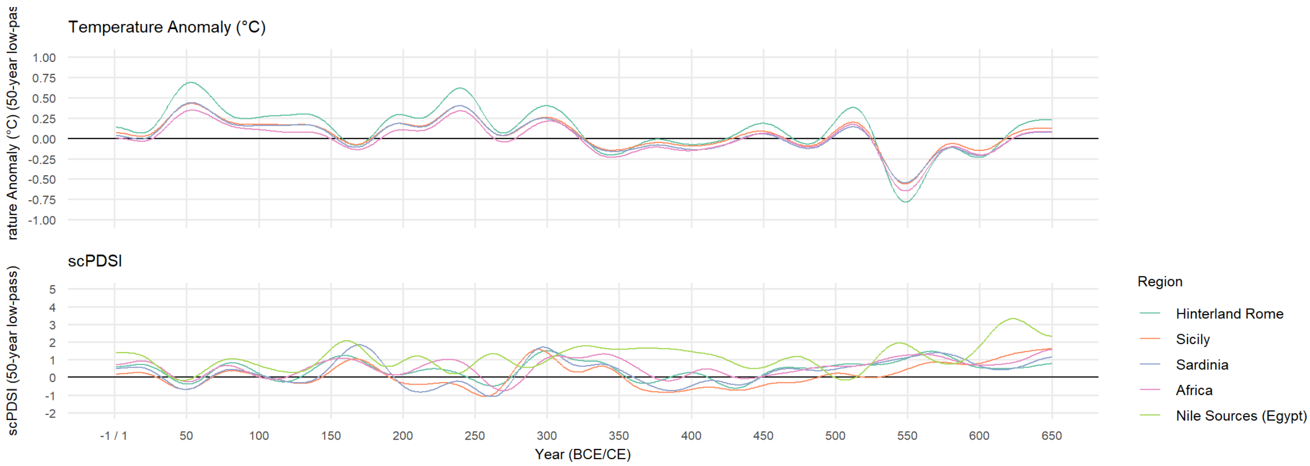

Figure 2. Palaeoclimatic indices (TA and scPDSI) for Rome's principal grain supply regions, 1–650 CE. All series represent regional averages smoothed using a 50 year lowpass filter. Temperature anomaly data derive from PHYDA, and scPDSI data derive from GEDA (Cook et al., 2024; Steiger et al., 2018).

In contrast to temperature anomalies, the 50 year lowpass filtered scPDSI reconstructions (Fig. 2) show greater interregional divergence in amplitude, frequency, and persistence of wetter and drier phases, in line with previous findings in palaeoclimatic literature demonstrating that hydroclimatic variability tends to display stronger regional differentiation than temperature (e.g., Finné et al., 2019; Labuhn et al., 2016). Up to c. 200 CE, most regions display broadly synchronous multi-decadal (c. 40 years) oscillations between wetter and near-average conditions. From the third century onwards, this regional synchrony weakens. During the fourth and early fifth centuries, the Nile sources experience a prolonged wetter phase, whereas Sicily and Sardinia show sustained slightly drier conditions and Africa and the hinterland of Rome fluctuate around near-average values. From the mid-fifth century, the Nile series shifts from sustained positive anomalies (wetter) to more pronounced multi-decadal oscillations, though generally remaining on the wetter side of the index. By contrast, the other study regions (Sicily, Sardinia, Africa, and the hinterland of Rome) display more moderate fluctuations, with interregional differences narrowing with a gradual convergence toward slightly wetter but near-average conditions.

3.3 Conceptual Framework and Analytical Strategy

To evaluate whether climate variability is systematically associated with the timing of historically attested food shortages in ancient Rome, we employ a twofold analytical strategy combining (1) multivariate regression analysis based on probit models and (2) a Monte Carlo simulation procedure.[3] These tests estimate the statistical associations between climatic variability and the years in which shortages are recorded, enabling an assessment of how environmental variability interacted with Rome's provisioning structures and whether particular climatic contexts systematically increased the likelihood of historically visible supply stress under specific provisioning configurations. The results are further interpreted at the level of

[3] All calculations and analyses were performed in the R statistical computing environment (R Core Team, 2026).

https://doi.org/10.5194/egusphere-2026-4354
Preprint. Discussion started: 28 July 2026

systemic interaction within a broader socio-ecological framework that recognises food shortages as outcomes of interdependent climatic, agrarian, institutional, and logistical processes (cf. White et al., 2023). Accordingly, climatic effects are evaluated in relation to Rome's production–provisioning system (Fig. 3), treating shortages as socio-natural outcomes mediated by institutional, economic, and political structures rather than as direct products of environmental shocks (Degroot, 2018; Degroot et al., 2021; Haldon et al., 2018; Slavin, 2016). At the same time, the historical visibility of these food shortages is shaped by processes of recording, narration, and preservation through which past events entered the surviving source tradition (Erdkamp, 2000, 2019; Van Bavel et al., 2019).

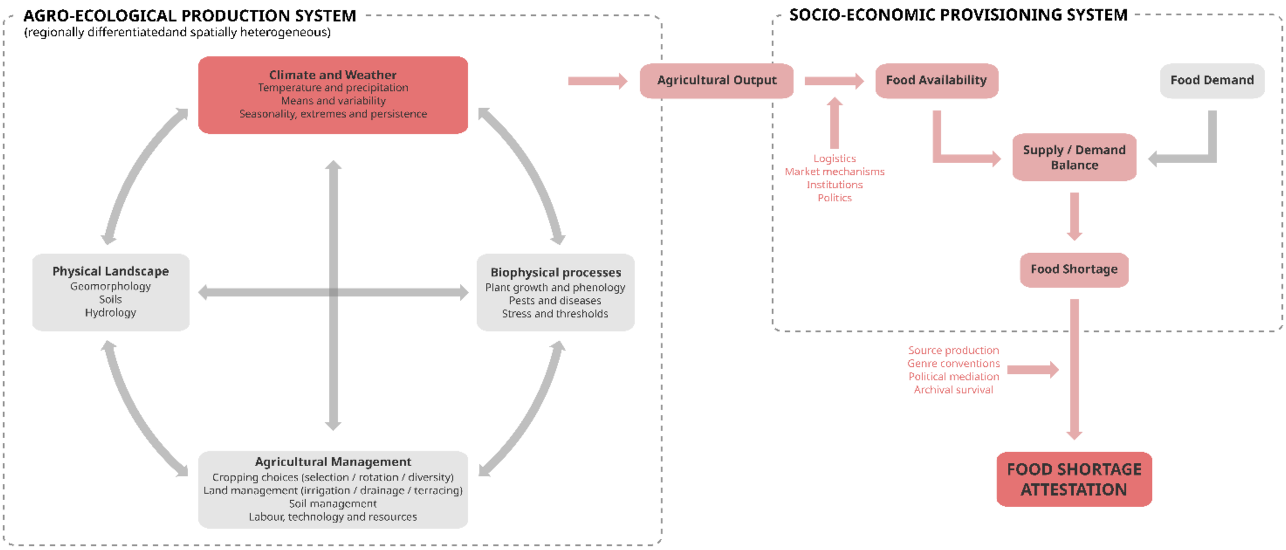

Figure 3. Conceptual framework linking climatic variability to attested food shortages in Rome, distinguishing between the agroecological production system (left) and the socio-economic provisioning system (right), through which agricultural food production is transformed into food availability and potential food shortages. Dark red elements represent variables included in the statistical analysis, light red elements represent mediating mechanisms considered in the interpretation and contextual analysis of the results. Grey elements denote structural components of the broader systemic context that are not directly operationalised in the analysis.

In line with the framework outlined above, the analysis explicitly situates climatic variability within Rome's broader institutional and logistical context, accounting for shifts in the role of its principal grain-supplying regions, namely the hinterland of Rome, Sicily, Sardinia, Africa, and Egypt. As Rome's reliance on different supply regions changed over time, so too did the climatic sensitivities that could have affected its food security, as these were contingent on the geographical configuration of its provisioning system. Accordingly, to ensure temporal consistency between the geographical configuration of the provisioning system and climatic variability, the analysis is conducted separately for three major chronological phases reflecting structural transformations in Rome's provisioning system:

1. **1–330 CE:** when Rome's provisioning reached its greatest geographic extent, sustained by grain imports from its hinterland, Sicily, Sardinia, Africa, and Egypt (22 attested shortages; average interval 15 years);

https://doi.org/10.5194/egusphere-2026-4354
Preprint. Discussion started: 28 July 2026

2. **331–450 CE:** when Africa, Sicily, Sardinia, and Rome's hinterland sustained the city following the redirection of Egyptian grain to Constantinople (13 attested shortages; average interval 9.2 years);
3. **451–650 CE:** when, after the Vandal conquest of Africa, Rome's provisioning relied increasingly on regional supplies from Italy, Sicily, and Sardinia, reflecting the contraction and decentralisation of the imperial grain supply system (20 attested shortages; average interval 10.0 years).

To capture both abrupt and prolonged climatic stress, such as persistent anomalies (e.g., multi-year cooling episodes, extended droughts), we include single-year values and multi-year rolling averages over 2, 3, 5, and 10 years, calculated for the preceding years only. These smoothed variables allow us to test whether food shortages were triggered not only by single-year climatic shocks, but also by the prolonged degradation of agrarian resilience under sustained stress. In a provisioning system reliant on grain storage, long-distance imports, and institutional coordination, as was the case in ancient Rome, such cumulative stress could gradually erode buffer capacity and increase the likelihood of food shortages only after considerable lag.

3.3.1 Probit Regression Analysis

The probit regression specification is used to model the probability that a documented food shortage occurred in a given year as a function of contemporaneous and preceding-year rolling average climatic conditions, thereby assessing the relative magnitude and direction of the association between single- or multi-year climatic conditions and the timing of recorded food shortages. The same specification is estimated separately for each of the three supply phases, consistent with the geographical configuration of the provisioning system, and for each temporal aggregation window (1, 2, 3, 5, and 10 years). For each supply phase, the model includes both linear and quadratic terms for TA and scPDSI. Linear terms capture directional effects, indicating whether warmer versus cooler or wetter versus drier conditions are associated with an increased or decreased likelihood of food shortages. Quadratic terms capture non-linear responses, testing whether extreme departures from average climatic conditions, irrespective of direction, are associated with heightened or reduced shortage risk. Climatic variables are standardised (z-scored) separately for each rolling window series to ensure comparability across predictors and to avoid scale-induced coefficient biases. All models are estimated using heteroskedasticity- and autocorrelation-consistent (HAC) standard errors. The full specification of the models is presented in Eq. (1).

$$Famine_t = \beta_0 + \sum_{r\in R_{TA}}\left(\beta_{1r}TA_{r,t} + \beta_{2r}TA^2_{r,t}\right) + \sum_{r\in R_{scPDSI}}\left(\beta_{3r}scPDSI_{r,t} + \beta_{4r}scPDSI^2_{r,t}\right) + \varepsilon_t \qquad (1)$$

where $Famine_t$ is a binary variable equal to 1 if a food shortage is attested in year t and 0 otherwise; β_0 is the intercept; β_1, β_2, β_3 and β_4 capture the linear and quadratic effects of temperature anomaly (TA) and self-calibrated Palmer Drought Severity Index (sc$PDSI$) values, respectively, for region r. The set R_{TA} includes the hinterland of Rome, Sicily, Sardinia, and Africa Proconsularis, while R_{scPDSI} comprises the same regions in addition to the Nile sources in year t. Finally, ε is the error term in

https://doi.org/10.5194/egusphere-2026-4354
Preprint. Discussion started: 28 July 2026

year *t*. The resulting regression coefficients, when statistically significant[4], indicate the direction and relative strength of the association between climatic conditions and attested food shortages. The sign indicates whether a given condition is associated with a higher or lower likelihood of a recorded shortage, while larger absolute values reflect stronger associations in the underlying latent propensity for food shortages.[5] Model diagnostics for all probit regression specifications are provided in Appendix A.

3.3.2 Monte Carlo Analysis

The Monte Carlo simulation, in turn, provides a complementary non-parametric test of whether shortage-year climatic conditions are anomalous, independent of directional modelling assumptions. Instead of estimating parametric relationships, it evaluates whether the distributions of TA and scPDSI values observed around attested shortage years differ significantly from those expected under random event occurrence, thereby assessing whether climatic conditions preceding documented food shortages fall outside the range expected from natural variability alone. The analyses are conducted separately for each supply phase, region, climatic variable, and temporal aggregation window. For each combination, we compare the observed distribution with 10,000 randomly generated event sequences that preserve the number of attested shortage events but randomise their temporal positions. Kernel density estimates are then calculated for the observed and simulated distributions, and the simulated densities are used to construct 95% confidence envelopes against which the observed density is evaluated.

3.4 Sensitivity Analyses

Sensitivity analyses were performed to evaluate the robustness of the principal findings to two potential sources of uncertainty: (1) uncertainty associated with palaeoclimatic reconstruction (Sect. 3.2) and (2) temporal variation in historical source coverage. To evaluate the effect of palaeoclimatic reconstruction uncertainty, the probit and Monte Carlo analyses were repeated using the 5th and 95th percentile estimates of the PHYDA temperature reconstruction ensemble. Equivalent uncertainty estimates are not available for the GEDA scPDSI dataset and could therefore not be included. To account for possible temporal variation in documentary coverage, the analyses were also repeated using a source coverage index derived from independent historical attestations of weather events, fires, and earthquakes (Table 2). In the probit analysis, the index was included as an additional categorical explanatory variable. In the Monte Carlo approach, the analysis was repeated using only years characterised by moderate-to-high source coverage (coverage index ≥ 2). Full methodological details are provided in Appendix B and C.

[4] Statistical significance indicates that the probability of observing such results by chance is, at most, 10% (“*”), 5% (“**”), and 1% (“***”).
[5] The probit model assumes the existence of an underlying continuous latent variable governing food shortages, which determines whether a shortage event is observed. The estimated coefficients capture the effect of climatic conditions on this latent propensity, which in turn translates into changes in the probability of observing a food shortage.

https://doi.org/10.5194/egusphere-2026-4354
Preprint. Discussion started: 28 July 2026

Table 2. Historical source coverage index based on the frequency of historical attestations of weather events (McCormick et al., 2012), fires (Canter, 1932), and earthquakes (Guidoboni et al., 1994) in successive 50 year periods for Rome and Italy. The total number of attestations was used to assign a source coverage index ranging from 0 (very low coverage) to 3 (high coverage).

Period (CE)	Weather	Fire	Earthquake	Total	Coverage Index
1–50	5	4	0	9	3
51–100	9	4	3	16	3
101–150	3	1	0	4	1
151–200	3	2	0	5	1
201–250	3	3	0	6	2
251–300	1	2	0	3	1
301–350	1	0	1	2	0
351–400	6	0	2	8	3
401–450	0	1	1	2	0
451–500	0	0	1	1	0
501–550	5	1	0	6	2
551–600	7	0	0	7	2
601–650	0	0	0	0	0

4 Statistical Assessment of Climate–Shortage Associations

4.1 Main Findings

Across the entire study period, the probit regressions provide no evidence for a stable, system-wide climate–shortage relationship (Fig. 4). Detectable associations are weak, heterogeneous across regions, and sensitive to the temporal window over which climatic conditions are summarised. For 1–330 CE, statistically significant associations are limited and concentrated mainly in multi-year windows, particularly for TA (3–5 year), but they vary in direction across regions. Sicily and Sardinia display contrasting non-linear responses at these scales. In Sicily, the likelihood of food shortages appears to be highest under sustained moderately warmer-than-average conditions and declines as temperature anomalies become more pronounced. By contrast, in Sardinia, food shortage risk increases under sustained cooling and, more generally, under more extreme climatic conditions (cooler but possibly also warmer). Africa Proconsularis shows a weaker but broadly similar sensitivity to multi-year temperature conditions, with some evidence that colder-than-average and more extreme values are associated with a higher likelihood of food shortages. The effects of prolonged dry or wet conditions (as captured by the scPDSI) on food shortages in this period are generally weaker and less consistent across regions and temporal windows. Rome's hinterland shows a modest scPDSI association at the longest (10 year) scale, where linear effects indicate increased shortage risk under prolonged wetter-than-average conditions. Elsewhere, these effects, although statistically detectable,

https://doi.org/10.5194/egusphere-2026-4354
Preprint. Discussion started: 28 July 2026

appear without persistent directionality. For Sardinia, negative quadratic effects at the 3 and 5 year scales indicate reduced food shortage risk during more extreme conditions (both TA and scPDSI), whereas the Nile sources show a weak positive quadratic effect at the 3 and 5 year scales, pointing to a limited and isolated sensitivity to prolonged scPDSI extremes in both drier and wetter conditions. The period 331–450 CE shows more frequent statistically detectable coefficients, but these remain spatially inconsistent and directionally unstable. Short-term (1 year) linear TA effects are most prominent, particularly in Rome's hinterland, Sardinia, and Africa Proconsularis. In Rome's hinterland, short-term warming is associated with an increased food shortage risk, whereas in Sardinia and Africa Proconsularis, cooling exerts relatively stronger adverse effects. Quadratic TA effects appear only at multi-year scales, with a positive response at 3 years in Sicily, indicating increased shortage risk under prolonged thermal extremes. In contrast, Sardinia and Africa Proconsularis display reduced risk during extremes but heightened vulnerability under more moderate yet persistent conditions. The influence of scPDSI on shortages remains comparatively weak and episodic, with isolated quadratic effects at particular windows but no sustained cross-regional structure. Sardinia and Sicily display positive quadratic responses at specific multi-year windows, respectively at the 3 and 10 year scale, indicating increased shortage risk under prolonged scPDSI extremes, whereas Africa Proconsularis shows a short-term (1 year) negative quadratic response. No consistent scPDSI associations are observed for Rome's hinterland. Only for 451–650 CE do clearer, more structured climatic associations emerge, particularly for TA. In Sicily, the combined linear and quadratic temperature effects indicate that cooler-than-average conditions are associated with increased shortage risk, but this appears to peak under moderate cooling and becomes weaker under more extreme conditions. The magnitude and statistical strength of this relationship become more pronounced in the multi-year windows, suggesting cumulative thermal stress rather than single-year shocks. Sardinia displays the opposite directional pattern. Here, the combined linear and quadratic TA effects indicate that warmer-than-average conditions are associated with increased shortage risk, and that this vulnerability is heightened under more extreme temperature deviations in both directions, though more strongly under warming. As in Sicily, the effect strengthens with increasing temporal aggregation, indicating heightened vulnerability under sustained thermal deviations. scPDSI effects remain less structured than those for TA. Still, Sicily shows a more persistent association with drier-than-average conditions across multiple temporal windows, whereas Sardinia exhibits a modest tendency toward increased risk under wetter multi-year conditions.

https://doi.org/10.5194/egusphere-2026-4354
Preprint. Discussion started: 28 July 2026

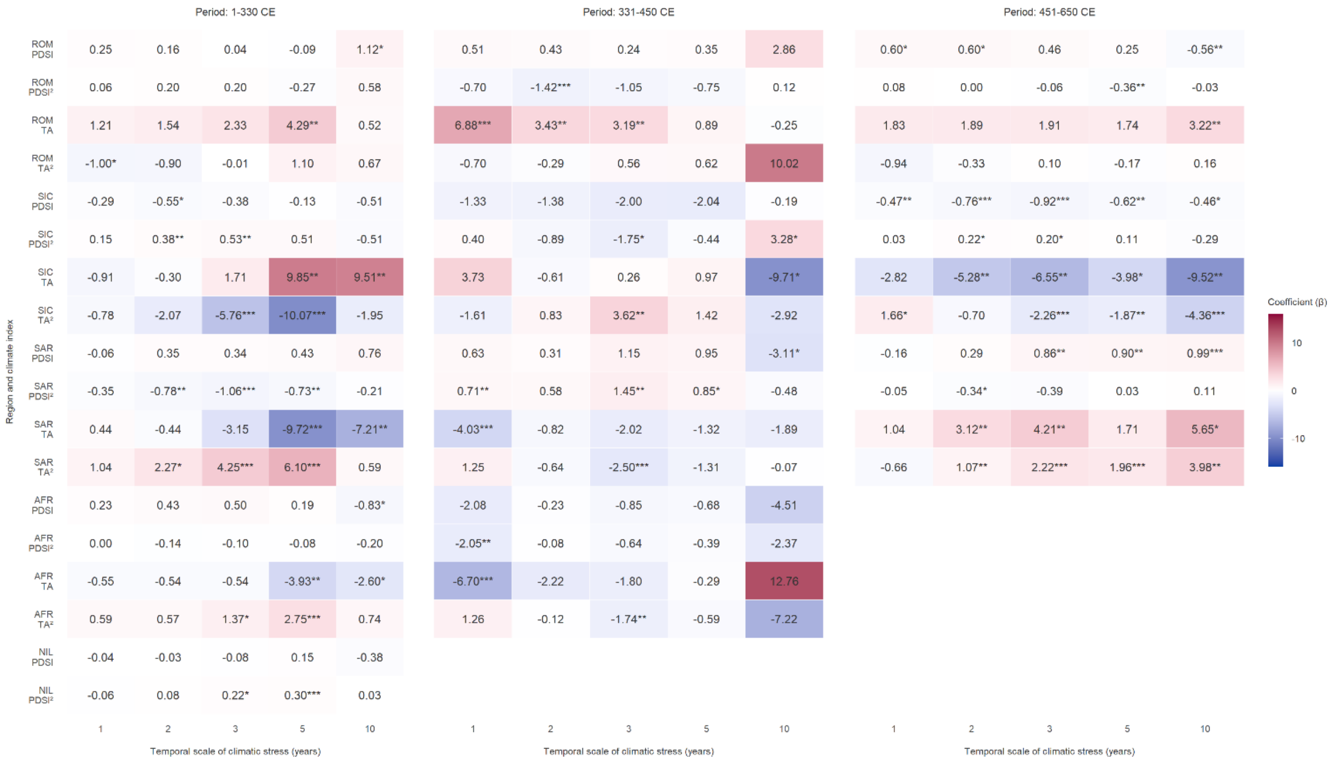

Figure 4. Probit regression coefficients for the relationship between climatic variability and the probability of food shortages in Rome across the three supply phases (1–330 CE, 331–450 CE, and 451–650 CE). Rows represent regions and climatic indices (TA = temperature anomaly, PDSI = scPDSI). Columns show temporal averaging windows. Reported values are coefficients. Asterisks (*, **, *) denote statistical significance at the 10%, 5%, and 1% levels, respectively. Model diagnostics (number of observations and pseudo-R² for each specification) are reported in Appendix A.**

The Monte Carlo simulations (Fig. 5) are consistent with the probit regression results in indicating region-, period-, and temporal-window-specific patterns in the association between climatic variables and attested food shortages. Overall, across most regions and periods, short-term windows (1–2 years) remain within expected ranges, suggesting that abrupt climatic shocks rarely translated directly into food shortages. Clearer deviations emerge primarily in multi-year windows and are most pronounced in the latest period. In 1–330 CE, deviations appear mainly in multi-year scPDSI windows. Specifically, 3–5 year (and, to a lesser extent, 10 year) scPDSI show an over-representation of shortage years under marginally wetter-than-expected conditions across most regions, except for the Nile sources. In 331–450 CE, departures from expectation likewise occur mainly in multi-year scPDSI windows but lack directional coherence. However, these deviations cluster around near-normal conditions and vary in direction across regions and window lengths. Rome shows a mild over-representation under near-normal to marginally wetter conditions in the 2–3 year windows, whereas Sicily and Sardinia shift toward modest over-representation under drier conditions in the 5–10 year windows. Africa displays a similar near-normal-to-slightly drier concentration over longer windows. More sustained and structured deviations become most clearly visible only in 451–650 CE. In this later period, multi-year scPDSI values for Rome's hinterland, and especially Sardinia, show shortages over-

https://doi.org/10.5194/egusphere-2026-4354
Preprint. Discussion started: 28 July 2026

represented under wetter-than-expected conditions (higher scPDSI) and under-represented under moderately drier conditions (lower scPDSI). TA display an even more pronounced pattern, with cooler-than-expected conditions being consistently over-represented in shortage years across all regions and temporal windows, and under-represented under slightly warmer-than-expected conditions, most clearly in Sardinia and Sicily in the multi-year evaluations.

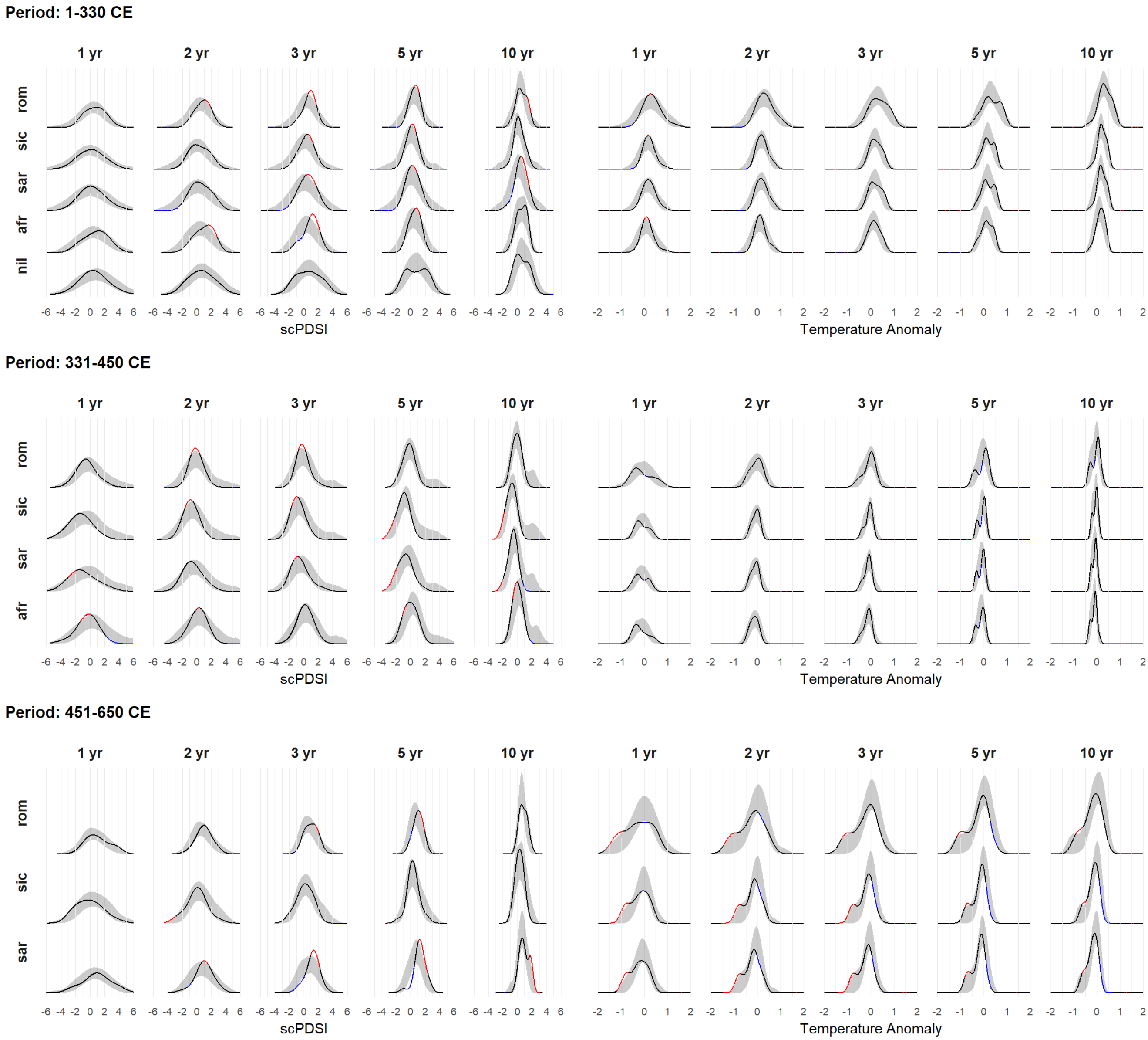

345 **Figure 5. Comparison of the distributions of climatic conditions during and preceding food shortages with Monte Carlo simulations based on 10,000 randomised event sequences for the three supply phases (1–330 CE, 331–450 CE, and 451–650 CE). Black curves represent the observed kernel density estimates, while grey bands indicate the 95% confidence envelopes derived from the randomised event sequences. Red and blue segments mark observed departures above or below the simulated confidence envelope, respectively.**

https://doi.org/10.5194/egusphere-2026-4354
Preprint. Discussion started: 28 July 2026

Taken together, the probit and Monte Carlo approaches identify 451–650 CE as the only period in which climatic associations with attested food shortages are more consistently detectable. Beyond this broad temporal agreement, the signal in both models remains fragmented and does not form a coherent or sustained pattern. Only for Sicily do the two methods produce a similar result: intermediate cooling in Sicily favoured food shortage at Rome, with the effect intensifying as the cooling continued. Extreme cooling may also have slightly favoured food shortage, but only in the same year. Overall, the absence of stable marginal probability effects (probit regression) and distributional concentrations (Monte Carlo) outside 451–650 CE, combined with period-, region-, and temporal window-specific associations between climate and attested food shortages, suggests that climate did not operate as a uniform or consistent trigger of food shortages in Rome.

4.2 Robustness of the Main Findings

The sensitivity analyses demonstrate that the principal findings are robust to both palaeoclimatic reconstruction uncertainty and temporal variation in historical source coverage.

For the sensitivity analyses based on the alternative (5th and 95th percentile) PHYDA temperature reconstructions, the results are largely consistent with those of the primary (ensemble-mean) analysis. In the probit models, 95.7–97.0% of coefficients retain the same direction of effect and 89.1–94.8% remain within the same p-value significance class across the two pairwise comparisons. The Monte Carlo analysis likewise demonstrates high agreement, with 90.5–91.0% of pointwise comparisons receiving the same confidence-envelope classification. The few instances of lower agreement are concentrated in the third supply phase, particularly for the hinterland of Rome and Sicily and at the 1, 3, and 10 year aggregation windows.

The sensitivity analyses accounting for historical source coverage likewise produced results broadly consistent with those of the primary analysis. For the probit models, 91.7% of coefficients retain the same direction of effect and 83.9% remain within the same p-value significance class. Coefficient differences are generally centred around zero, with the few larger deviations observed for temperature anomaly predictors in the second supply phase (331–450 CE), particularly for the hinterland of Rome, Sicily, and Sardinia at the 10 year aggregation window. Notably, these larger deviations coincide with the supply phase showing the greatest variation in the historical source coverage (Table 2), suggesting that the estimated climate–shortage relationships during this interval may be comparatively more sensitive to documentary visibility than those obtained for the earlier and later phases. The Monte Carlo analysis likewise demonstrates high agreement, with 87.3% of pointwise comparisons receiving the same confidence envelope classification. Although lower agreement is slightly more pronounced for scPDSI than for temperature anomaly, it shows no systematic concentration across supply phases, supply regions, or temporal aggregation windows. Overall, both the probit robustness check and alternative Monte Carlo analysis suggest that mitigating the effects of heterogeneous source coverage does not materially alter the main conclusions of this study.

https://doi.org/10.5194/egusphere-2026-4354
Preprint. Discussion started: 28 July 2026

Detailed sensitivity analysis results are provided in Appendix B and C.

5 Climate and Resilience of Rome's Food Supply System

Rather than indicating a consistent and systematic climate–food shortage relationship, the analysis suggests that, within the limits of the available proxy evidence, climatic variability did not automatically translate into food shortages in Rome and does not emerge as a consistent predictor of food shortage years. Instead, any climatic signal is conditional upon the specific configuration of Rome's provisioning system. More concretely, this interpretation is supported by the results of both the probit models and the Monte Carlo simulations: (1) the probit models yield few coefficients that are stable in sign and significance across regions and temporal window specifications in 1–330 and 331–450 CE, with effects appearing mainly as scattered multi-year temperature anomaly (TA) terms with only limited short-term and hydroclimatic signals; and (2) the Monte Carlo tests show shortage-year climatic conditions largely indistinguishable from random event expectations in these earlier phases, with sustained departures from the null envelope emerging primarily in 451–650 CE, most clearly in the widespread over-representation of cooler-than-expected conditions across regions and window lengths, alongside a weaker under-representation of slightly warmer conditions. During the 1–330 CE phase, neither short-term climatic shocks nor sustained multi-year anomalies show consistent or regionally coherent associations with recorded shortages.

Our thesis states that the absence of systematic and coherent associations between climatic variability and attested food shortages is not merely coincidental but instead reflects underlying ecological, institutional and logistical dynamics. As argued throughout the paper, Rome's reliance on multiple ecological zones appears to have limited systemic vulnerability even during periods of pronounced climatic variability. This ecological differentiation is particularly evident in Egypt, the principal grain supplier of the early Empire, whose flood-based production regime was structurally distinct from Mediterranean rain-fed cereal systems. Since Egyptian agriculture depended on monsoon-driven Nile inundation, its production variability was asynchronous with climatic conditions in other supply regions. Also here, the absence of a consistent association between Nile-source hydroclimatic variability (represented by scPDSI data extracted for the Nile catchment) and shortage years suggests that interannual flood variability was not systematically transmitted into Rome's shortage record. This decoupling was reinforced by the structure of the Egyptian fiscal system, which assessed land tax per unit of cultivated land rather than as a percentage of annual yield and whose fiscal structure was geared toward predictable extraction (Erdkamp, 2013). Although Nile floods were far from uniform on a year-to-year basis, the combination of flood-based irrigation and institutional coordination likely enhanced the buffering capacity of Rome's supply network. In this high-integration phase, climatic stress was certainly not absent; rather, its effects were more likely absorbed or redistributed within an ecologically diversified and institutionally integrated provisioning system. Following the redirection of Egyptian grain to Constantinople in the early fourth century CE, Rome's supply network contracted but remained distributed across diverse ecological settings. Although attested shortages became more frequent (see Sect. 3.1), climatic associations remain weak and inconsistent, suggesting that the increased crisis frequency cannot be straightforwardly attributed to climatic variability. Indeed, while the 331–450 CE phase produces more statistically detectable probit coefficients, these lack cross-regional coherence, and the Monte Carlo distributions remain largely within the simulated confidence bands. It is important to note, however, that this interpretation should be viewed in light of the sensitivity analyses (see Appendix C), which indicate that the estimated climatic relationships for this phase may be more sensitive to temporal variation in historical source coverage than those of the preceding and succeeding supply phases.

Only after the mid-fifth century, when provisioning became increasingly regionalised following the loss of Africa, does a more coherent, though still modest, climatic signal become detectable. As Rome increasingly relied on regional Italian and insular production (particularly Sicily and Sardinia), its capacity to offset regional anomalies weakened, increasing its sensitivity to synchronous stress. In other words, similar levels of climatic variability were more likely to translate into shortages in this later period because Rome's supply network became more geographically concentrated.

Overall, neither hydroclimatic variability nor temperature anomalies consistently emerge as direct or reliable predictors of food shortage years in Rome. Where associations appear, they are region-specific and temporally heterogeneous, underscoring that climatic influence operated through differentiated ecological and production regimes rather than as a uniform Mediterranean-wide force. Hydroclimatic variability appears comparatively spatially heterogeneous and episodic, reducing the likelihood of synchronised failure across supply regions and suggesting that geographic diversification functioned as a structural stabiliser within Rome's provisioning network. Moreover, such variability may have been partly anticipated within Mediterranean rain-fed agriculture through adaptive strategies such as flexible sowing regimes, crop diversification, and storage buffers. Temperature variability, by contrast, shows greater spatial coherence and temporal stability. If temperature was generally experienced as more stable than hydroclimate, sustained deviations may have posed more systemic agricultural challenges to farmers. Notably, the strongest multi-region clustering in the Monte Carlo analysis concerns temperature in 451–650 CE, whereas hydroclimate produces at most weak, localised departures; this asymmetry strengthens the inference that spatially coherent thermal anomalies were more capable of generating synchronous stress across Rome's reduced supply zone than regionally differentiated hydroclimatic variability. The scope of these findings is conditioned by the resolution of the climatic indices employed, which capture seasonal-scale variability rather than the locally specific interplay between broader climatic background conditions and short-term weather extremes. Harvest outcomes depended not only on seasonal trends but also on phenological sensitivities at critical stages (such as autumn sowing, spring growth, and summer harvest) during which brief extremes, like late frosts, sudden droughts, heat spikes, or excessive rainfall could disrupt yields, damage crops, or increase the risk of fungal infection and post-harvest losses (Heinrich and Hansen, 2021; Watson et al., 2001).

https://doi.org/10.5194/egusphere-2026-4354
Preprint. Discussion started: 28 July 2026

While it is without doubt that climate affected agricultural output, harvest fluctuations did not automatically translate into food shortages. The critical question was not only how much grain was produced, but how effectively it was extracted, stored, transported, and distributed. In other words, the conversion of physical availability into socially available food depended on the political and administrative organisation of Rome's provisioning system. The Roman grain system was not a passive conduit of grain flows but a politically structured system of taxation, storage, routing, distribution, and release policies. As such, provisioning outcomes were shaped as much by administrative capacity, fiscal priorities, and political intervention as by harvest conditions. The absence of a consistent climate–food shortage relationship suggests that Rome's food system and its related administrative coordination and logistical capacity (including mechanisms of taxation, storage, and redistribution) were generally effective in absorbing regional agrarian variability. Climatic shocks did not automatically produce shortages; only in the period 451–650 CE, when geographic diversification contracted and institutional coordination weakened, did environmental variability become more visibly associated with shortage. Moreover, historical evidence repeatedly links episodes of food shortage in Rome to political intervention and logistical disruption, with emperors intervening directly in storage, release, or symbolic displays of abundance (e.g., blockades, conflicts over shipments, and the instrumentalisation of grain as leverage), rather than to a climatic trigger (Erdkamp, 2005; Linn, 2012; Wijnendaele, 2019).[6] In this sense, climate can be best understood as a background stressor whose historical consequences depended on whether institutional integration, logistical mechanisms, and political stability dampened, redistributed, or amplified production shortfalls. Only when this institutional integration weakened in 451–650 CE does climatic variability become more readily detectable in association with shortage years.

Importantly, these findings must be read in light of the nature of the historical record itself. Documented shortages come from sources whose principal purpose was not the systematic documentation of subsistence conditions, but the narration of political, moral, and theological developments (Erdkamp, 2000, 2019; Van Bavel et al., 2019). Reported shortages should therefore be understood as narratively framed observations shaped by the political and ideological contexts in which they were written, rather than neutral records of food insecurity. Their temporal distribution reflects not only the occurrence of subsistence pressures, but also the selective processes of recording, transmission, and survival that shape the extant evidence. As such, the absence of a recorded shortage cannot be equated with the absence of subsistence stress. The dataset used here should thus be understood not as a comprehensive catalogue of all historical food shortages, but as a conservative estimate of shortage visibility rather than a direct measure of underlying scarcity frequency. That said, the sensitivity analyses indicate that broad temporal variation in historical source coverage does not substantially alter the overall analytical patterns (Appendix C). Because food shortages are operationalised here as discrete binary events, the analysis necessarily abstracts from variation in severity, duration, and social impact (Van Bavel et al., 2019). The results should therefore be interpreted as indicating a lack of systematic statistical associations between climatic conditions and the timing of historically visible

[6] E.g., Suetonius, *Calig.* 26.4; Tacitus, *Ann.* 15.18.2; Herodian 1.12.2–4; Cassius Dio 73.13.1) (Erdkamp, 2005; Taylor, 2010).

https://doi.org/10.5194/egusphere-2026-4354
Preprint. Discussion started: 28 July 2026

supply disruptions. While such episodes do not necessarily capture the full extent of food insecurity in Rome, the absence of consistent associations between climatic conditions and documented food shortages suggests that climate alone was insufficient to systematically trigger food shortages in ancient Rome, at least until the Early Middle Ages.

6 Conclusions

This paper statistically examined whether climatic variability was systematically associated with historically attested food shortages in Rome between 1 and 650 CE. By combining probit regression models with Monte Carlo simulations, and by embedding these statistical tests within a historically grounded reconstruction of Rome's provisioning system, we assessed under what structural conditions climatic variability translated into historically attested food shortages in Rome. Across two complementary analytical strategies, the results show no stable, system-wide association between climatic conditions and the timing of recorded food shortages. During the Imperial (1–330 CE) and Late Antique (331–450 CE) phases, neither short-term climatic variability nor sustained multi-year anomalies reveal consistent or regionally coherent effects. Probit coefficients remain weak, heterogeneous, and sensitive to temporal specification, whereas Monte Carlo simulations indicate that shortage years fall largely within the range expected under random variability. In this high-integration phase, Rome's geographically diversified supply network appears to have effectively absorbed interannual climatic variability. The absence of systematic climate–shortage coupling underscores the stabilising role of ecological diversification and administrative coordination within Rome's grain supply system. Only in the period 451–650 CE, following the further contraction of Rome's provisioning network after the loss of Africa, does a more coherent climatic pattern become detectable. Both the probit regression and Monte Carlo analysis for this later phase indicate clearer and more structured temperature effects, yet these remain regionally differentiated in their directional responses and do not constitute a uniform system-wide climatic trigger. Only for Sicily did both methods indicate that cooler-than-average conditions (over both the short and long term) were associated with an increased probability of food shortage in Rome. All this shows that climatic variability did not automatically generate food crises in Roman times. Only under conditions of reduced diversification and weakened institutional resilience did climatic signals become more discernible in the historical record. Climatic stress formed part of the environmental backdrop, but its translation into food shortage depended on the functioning of Rome's grain administration and the stability of its supply networks. As such, this regional differentiation argues against the uncritical application of coarse-grained climatic periods, such as the Roman Climatic Optimum, to the Roman empire as a whole.

More broadly, these findings demonstrate the necessity of analysing palaeoclimatic evidence within historically specific production and provisioning structures. Statistical associations between climate variability and societal outcomes cannot be interpreted in isolation from agrarian regimes, fiscal institutions, and logistical systems through which environmental variability was filtered. By distinguishing between probability effects (probit) and distributional clustering (Monte Carlo), this study shows that climatic influence was conditional, context-dependent, and structurally mediated. The Roman

https://doi.org/10.5194/egusphere-2026-4354
Preprint. Discussion started: 28 July 2026

provisioning network functioned as a shock-absorbing system rather than a passive reflection of environmental change. When food shortages occurred, they appear less as inevitable outcomes of climatic anomalies than as moments when socio-political mechanisms of mediation proved insufficient to offset regional stress. Climate variability shaped the margins of subsistence risk; whether that risk materialised as food shortage depended on the configuration and resilience of Rome's provisioning system at a given historical moment. When geographic diversification and administrative coordination remained strong, environmental variability was largely absorbed; when buffering capacity weakened, climatic signals became more discernible. In this respect, the study contributes to debates on climate and societal change in the Roman world by shifting the analytical focus from whether climate "mattered" to how institutional structures conditioned its effects.

Appendix A: Model Diagnostics for Probit Regression Specifications

Supply Phase	Temporal window (years)	Number of years[1]	Food shortage observations[2]	Pseudo-R2 (McFadden)
1–330 CE	1	330	22	0.084
	2	329	22	0.135
	3	328	22	0.191
	5	326	22	0.247
	10	321	18	0.285
331–450 CE	1	120	13	0.392
	2	120	13	0.285
	3	120	13	0.325
	5	120	13	0.278
	10	120	13	0.539
451–650 CE	1	200	20	0.182
	2	200	19	0.240
	3	200	18	0.294
	5	200	18	0.248

[1] Number of yearly observations included in each model specification. For the period 1–330 CE, the number of observations decreases with increasing temporal window length because rolling averages require preceding years for which no climatic data are available prior to 1 CE. For the later periods, preceding-year climatic values outside the focal period are included.

[2] Number of years in which a food shortage is recorded. The number of events can vary across temporal windows due to the loss of early observations when constructing rolling averages.

https://doi.org/10.5194/egusphere-2026-4354
Preprint. Discussion started: 28 July 2026

Appendix B: Sensitivity Analysis of the PHYDA Temperature Anomaly Reconstruction Ensemble

Appendix B presents the sensitivity analyses used to evaluate the robustness of the primary results to uncertainty in the PHYDA temperature anomaly reconstruction ensemble. The complete probit and Monte Carlo workflows were repeated using the ensemble-mean (TA mean), 5th percentile (TA P05), and 95th percentile (TA P95) PHYDA temperature reconstructions, thereby representing conservative lower and upper bounds of plausible temperature histories. Equivalent uncertainty estimates are not available for the GEDA scPDSI dataset and could therefore not be incorporated into the sensitivity analyses.

Probit Regression

For the probit sensitivity analysis, the complete modelling workflow was repeated independently for each PHYDA temperature reconstruction: TA mean, TA P05, and TA P95. In each case, the original model specification, event chronology, temporal windows, and GEDA scPDSI predictors were kept unchanged, while only the PHYDA temperature reconstruction was substituted. To assess robustness, regression coefficients obtained from the alternative probit models were compared with those from the original ensemble-mean model. Consistency was evaluated by assessing whether corresponding coefficients retained (1) the same direction of effect (positive or negative) and (2) the same p-value significance class (<0.01, 0.01–0.05, 0.05–0.10, or ≥0.10). Changes in coefficient magnitude were quantified as the absolute differences between corresponding coefficient estimates. Summary statistics are presented in Table B1, while coefficient differences relative to the ensemble-mean model and their summary statistics are shown in Figures B1 and B2.

Across the 230 matched regression coefficient pairs in each comparison, coefficients retain the same direction of effect in 97.0% of comparisons between the TA mean and TA P05 models, and in 95.7% of comparisons between the TA mean and TA P95 models (Table B1). Consistency in p-value significance class is slightly lower, at 94.8% for TA mean versus TA P05 and 89.1% for TA mean versus TA P95. Median absolute coefficient differences remain small, amounting to 0.05 for the TA P05 comparison and 0.08 for the TA P95 comparison. The corresponding interquartile ranges (0.01–0.19 and 0.01–0.25 for TA P05 and TA P95, respectively) and maximum ranges (2.39 and 4.28, respectively) indicate that larger deviations are confined to a small number of coefficients, particularly in the TA P95 comparison. Figures B1 and B2 likewise shows that coefficient differences cluster closely around zero across temporal aggregation windows, supply phases, supply regions, and climatic variables, with only a limited number of outlying comparisons.

Table B1. Summary statistics of the sensitivity analysis of the probit regression models comparing results obtained using ensemble-mean, 5th percentile, and 95th percentile of the temperature anomaly reconstructions from PHYDA. Same p-value significance class (%) denotes the percentage of coefficients assigned to the same statistical significance class between the compared models ($p < 0.01$, $0.01 \leq p < 0.05$, $0.05 \leq p < 0.10$, and $p \geq 0.10$).

Statistic	TA mean vs TA P05	TA mean vs TA P95

Number of coefficient pairs compared	230	230
Same coefficient direction (%)	97.0	95.7
Same p-value significance class (%)	94.8	89.1
Median absolute coefficient difference	0.05	0.08
IQR absolute coefficient difference	0.01–0.19	0.01–0.25
Range absolute coefficient difference	0.00–2.39	0.00–4.28

https://doi.org/10.5194/egusphere-2026-4354
Preprint. Discussion started: 28 July 2026

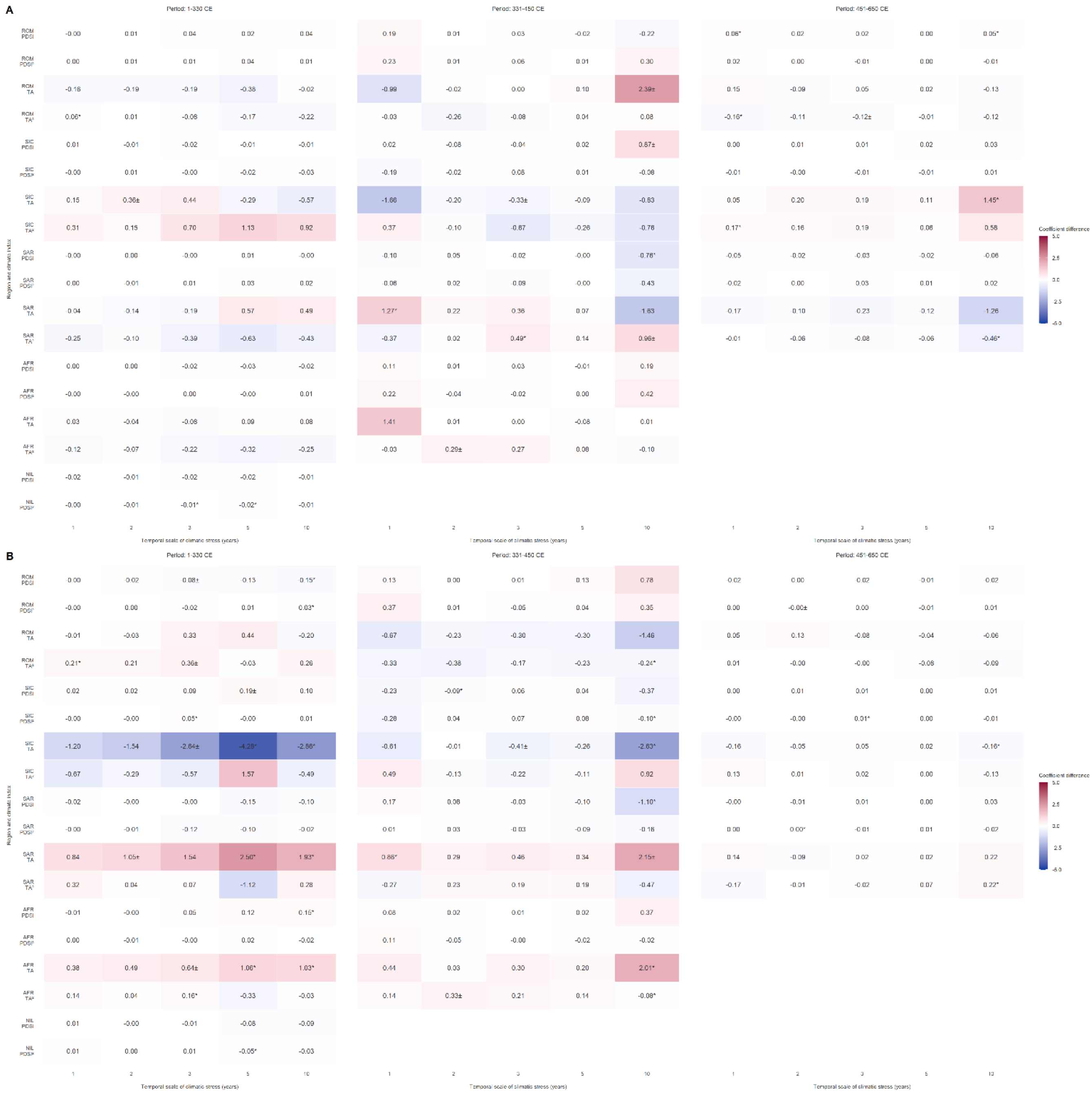

Figure B1. Differences in probit regression coefficients between models using the PHYDA ensemble-mean temperature reconstruction and models using the (A) 5th percentile and (B) 95th percentile ensemble reconstructions. Rows represent regions and climatic indices (TA = temperature anomaly; PDSI = scPDSI). Columns show temporal averaging windows (1–10 years). Reported values are the differences in regression coefficients relative to the ensemble-mean model (alternative reconstruction − ensemble mean). An asterisk (*) indicates that the coefficient belongs to a different p-value significance class (<0.01, 0.01–0.05, 0.05–0.10, or ≥0.10) than in the ensemble-mean model. An exclamation mark (!) indicates that the coefficient changed direction (i.e. from positive to negative or vice versa).

https://doi.org/10.5194/egusphere-2026-4354
Preprint. Discussion started: 28 July 2026

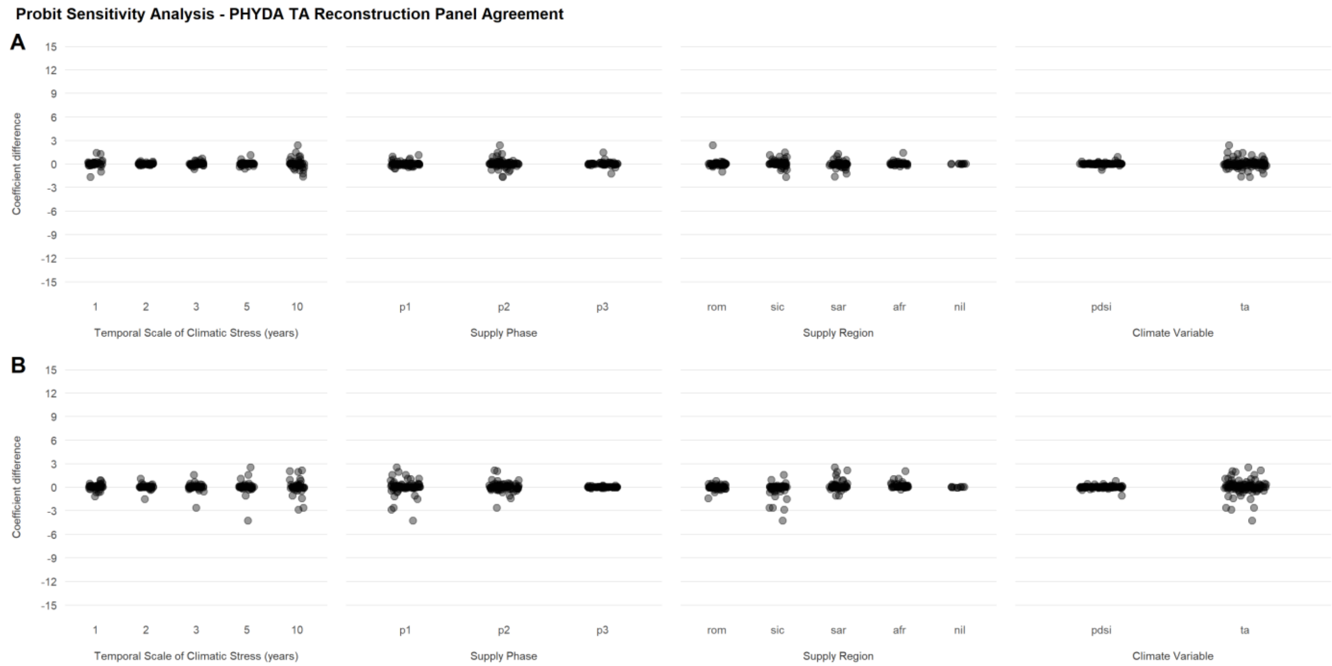

Figure B2. Distribution of the differences in probit regression coefficients between models using the PHYDA ensemble-mean temperature reconstruction and models using the (A) 5th percentile and (B) 95th percentile ensemble reconstructions. Points are grouped by temporal averaging window, supply phase, supply region, and climatic variable.

Monte Carlo Approach

For the Monte Carlo analysis, the complete simulation workflow was repeated independently for each PHYDA temperature reconstruction: TA mean, TA P05, and TA P95. In each case, the same event chronology, supply phases, supply regions, temporal aggregation windows, and simulation settings were used, with only the temperature reconstruction varied. To assess robustness, the observed kernel density estimates were evaluated point-by-point against the corresponding Monte Carlo simulation envelope, with each point classified as lying below, above, or within the envelope. Agreement was then quantified by comparing these classifications across the three temperature reconstructions. Overall agreement is the percentage of all pointwise comparisons for which the ensemble-mean, 5th percentile, and 95th percentile reconstructions produced the same confidence envelope classification. Agreement was also calculated separately for each combination of supply phase, supply region, and temporal aggregation window (hereafter referred to as panel). Panel agreement was summarised using the median, interquartile range (IQR), and range (Table B2). Panel-specific agreement values and summary statistics for all 55 panels are presented in Figures B3 and B4, respectively.

The Monte Carlo classifications are generally consistent between the ensemble-mean PHYDA temperature reconstruction and both the 5th and 95th percentile ensemble reconstructions. Overall agreement is 90.5% for the TA mean versus TA P05 comparison and 91.0% for the TA mean versus TA P95 comparison, indicating that the alternative temperature

https://doi.org/10.5194/egusphere-2026-4354
Preprint. Discussion started: 28 July 2026

reconstructions produce the same confidence envelope classification in most pointwise comparisons (Table B2). Agreement is likewise high at the panel level, with median agreement values of 92.4% (IQR: 86.0–94.7%) and 91.8% (IQR: 89.4–94.8%) for the TA mean versus TA P05 and TA mean versus TA P95 comparisons, respectively. Although panel-level agreement ranges from 77.4% to 97.9% for TA P05 and from 72.9% to 97.7% for TA P95, the panel-specific heatmaps (Fig. B3) show that lower agreement are confined to a relatively small number of sensitivity-analysis panels, primarily involving the third supply phase, particularly for the hinterland of Rome and Sicily and at the 1, 3, and 10 year aggregation windows. Figure B4 further demonstrates that these lower-agreement panels represent isolated cases, with most panel comparisons clustering above 90% agreement irrespective of temporal aggregation window, supply phase, or supply region.

Table B2. Summary statistics of the agreement between Monte Carlo simulation envelopes obtained using the ensemble-mean, 5th percentile, and 95th percentile of the temperature anomaly reconstructions from PHYDA.

Statistic	TA mean vs TA P05	TA mean vs TA P95
Number of panel pairs compared	55	55
Number of pointwise pairs compared	56,320 (1,024 per panel)	56,320 (1,024 per panel)
Overall agreement (%)	90.5	91.0
Median panel agreement (%)	92.4	91.8
IQR panel agreement (%)	86.0–94.7	89.4–94.8
Range panel agreement (%)	77.4–97.9	72.9–97.7

https://doi.org/10.5194/egusphere-2026-4354
Preprint. Discussion started: 28 July 2026

605 **Figure B3. Heatmaps showing the percentage agreement in Monte Carlo confidence envelope classification between models using the PHYDA ensemble-mean temperature reconstruction and models using the (A) 5th percentile and (B) 95th percentile ensemble reconstructions. Rows represent regions and climatic indices (TA = temperature anomaly; PDSI = scPDSI). Columns show temporal averaging windows (1–10 years).**

https://doi.org/10.5194/egusphere-2026-4354
Preprint. Discussion started: 28 July 2026

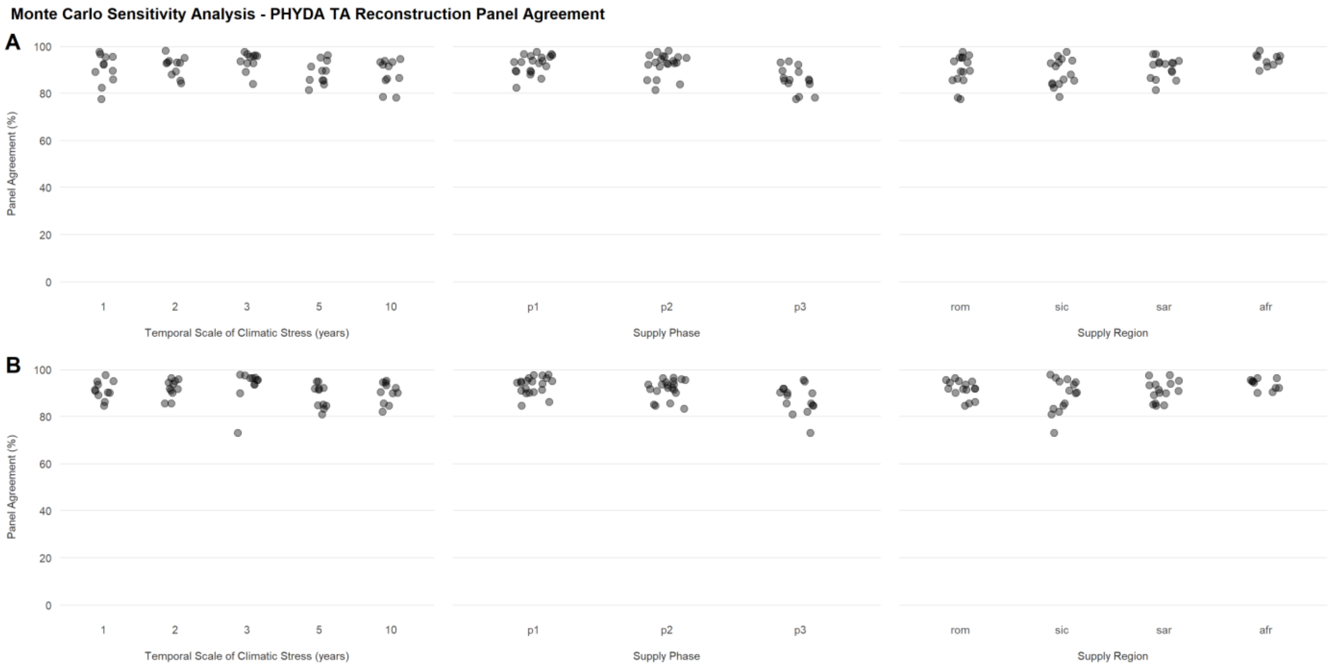

Figure B4. Distribution of Monte Carlo panel-level agreement between models using the PHYDA ensemble-mean temperature reconstruction and models using the (A) 5th percentile and (B) 95th percentile ensemble reconstructions. Points are grouped by temporal averaging window, supply phase, and supply region.

Appendix C: Sensitivity Analysis Accounting for Historical Source Coverage

Appendix C presents the sensitivity analyses undertaken to evaluate the robustness of the primary results to potential biases arising from temporal variation in historical source coverage. Separate sensitivity analyses were performed for the probit regression and Monte Carlo approaches using an index of general historical visibility based on weather events, fires, and earthquakes attested in historical literature (Table 2 in the main text). Because the index is derived from multiple categories of historical events rather than food shortages themselves, it is unlikely to be endogenous to the recording of food shortages. It therefore provides a suitable independent proxy for temporal variation in source coverage.

$$E(\varepsilon_t \mid X_t) \neq 0 \qquad \text{(C1)}$$

where X_t denotes the climatic regressors (TA, scPDSI, and their quadratic terms), while ε_t captures the omitted variation associated with source coverage. Under these circumstances, the estimated coefficients may reflect not only the relationship between climate variability and food shortages, but also temporal variation in the probability that food shortages are historically recorded.

https://doi.org/10.5194/egusphere-2026-4354
Preprint. Discussion started: 28 July 2026

To evaluate whether such reporting bias materially influences the estimated climate–food shortage relationships, the original probit model specifications were repeated with the inclusion of the source coverage index as an additional categorical explanatory variable, thereby directly accounting for temporal variation in documentary coverage over the study period. The complete chronological series was retained, while the original climatic variables, temporal aggregation windows, supply phases, supply regions, and model specification remained unchanged. Incorporating the source coverage index directly accounts for temporal variation in documentary coverage throughout the study period and reduces the risk that differences in documentary preservation, rather than climatic variability, drive the estimated relationships between climate variability and attested food shortages. To assess robustness, regression coefficients obtained from the source-coverage-adjusted models were compared with those from the original models. Consistency was evaluated by assessing whether corresponding coefficients retained (1) the same direction of effect (positive or negative) and (2) the same p-value significance class (<0.01, 0.01–0.05, 0.05–0.10, or ≥0.10). Changes in coefficient magnitude were quantified as the absolute differences between corresponding coefficient estimates. Summary statistics are presented in Table C1, while coefficient differences relative to the original model and their summary statistics are shown in Figures C1 and C2.

Across the 230 matched regression coefficient pairs, coefficients retain the same direction of effect in 91.7% of comparisons between the original model and the model including the historical source coverage index (Table C1). Consistency in p-value significance class is somewhat lower, at 83.9%. Nevertheless, median absolute coefficient differences remain modest (0.14), with an interquartile range of 0.04–0.58 and a maximum range of 12.25. Figures C1 and C2 show that across all temporal aggregation windows, supply phases, supply regions, and climatic variables, most coefficients change only modestly and are centred around zero. Larger deviations, even though confined to a limited number of coefficients, are concentrated primarily in the temperature anomaly predictors for the second supply phase (331–450 CE), particularly for the hinterland of Rome, Sicily and Sardinia at the 10 year aggregation window. Notably, these larger deviations coincide with the supply phase showing the greatest variation in the historical source coverage (Table 2 in the main text), suggesting that the estimated climate–shortage relationships during this interval may be comparatively more sensitive to documentary visibility than those obtained for the earlier and later phases.

Table C1. Summary statistics of the sensitivity analysis of the probit regression models comparing the original models with models including the historical source coverage index. Same p-value significance class (%) denotes the percentage of coefficients assigned to the same statistical significance class between the compared models ($p < 0.01$, $0.01 \leq p < 0.05$, $0.05 \leq p < 0.10$, and $p \geq 0.10$).

Statistic	Original vs Historical Source Coverage
Number of coefficient pairs compared	230
Same coefficient direction (%)	91.7
Same p-value significance class (%)	83.9
Median absolute coefficient difference	0.14

IQR absolute coefficient difference	0.04–0.58
Range absolute coefficient difference	0.00–12.25

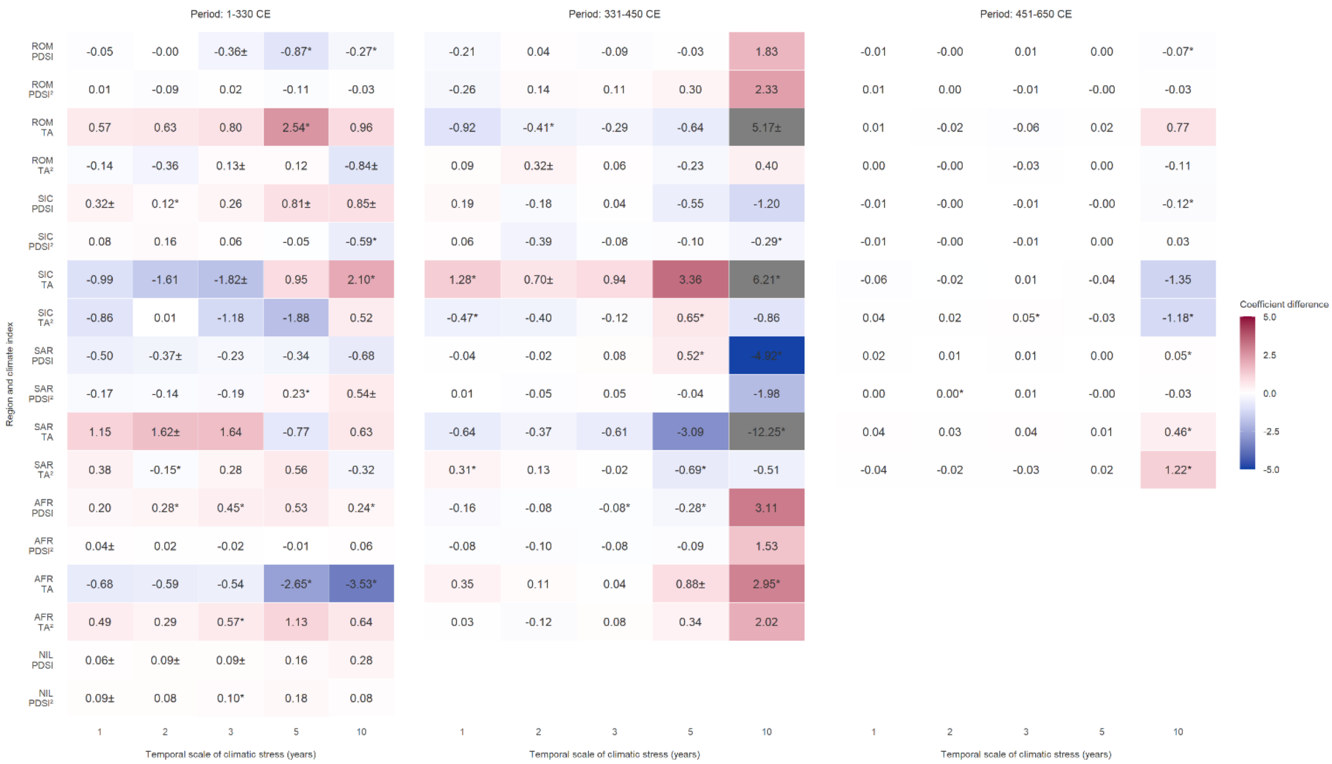

655 **Figure C1. Differences in probit regression coefficients between the main model and the model including the historical source coverage index. Rows represent regions and climatic indices (TA = temperature anomaly; PDSI = scPDSI). Columns show temporal averaging windows (1–10 years). Reported values are the differences in regression coefficients relative to the ensemble-mean model (alternative reconstruction − ensemble mean). An asterisk (*) indicates that the coefficient belongs to a different p-value significance class (<0.01, 0.01–0.05, 0.05–0.10, or ≥0.10) than in the ensemble-mean model. An exclamation mark (!) indicates**
660 **that the coefficient changed direction (i.e. from positive to negative or vice versa). Outliers are marked in grey.**

https://doi.org/10.5194/egusphere-2026-4354
Preprint. Discussion started: 28 July 2026

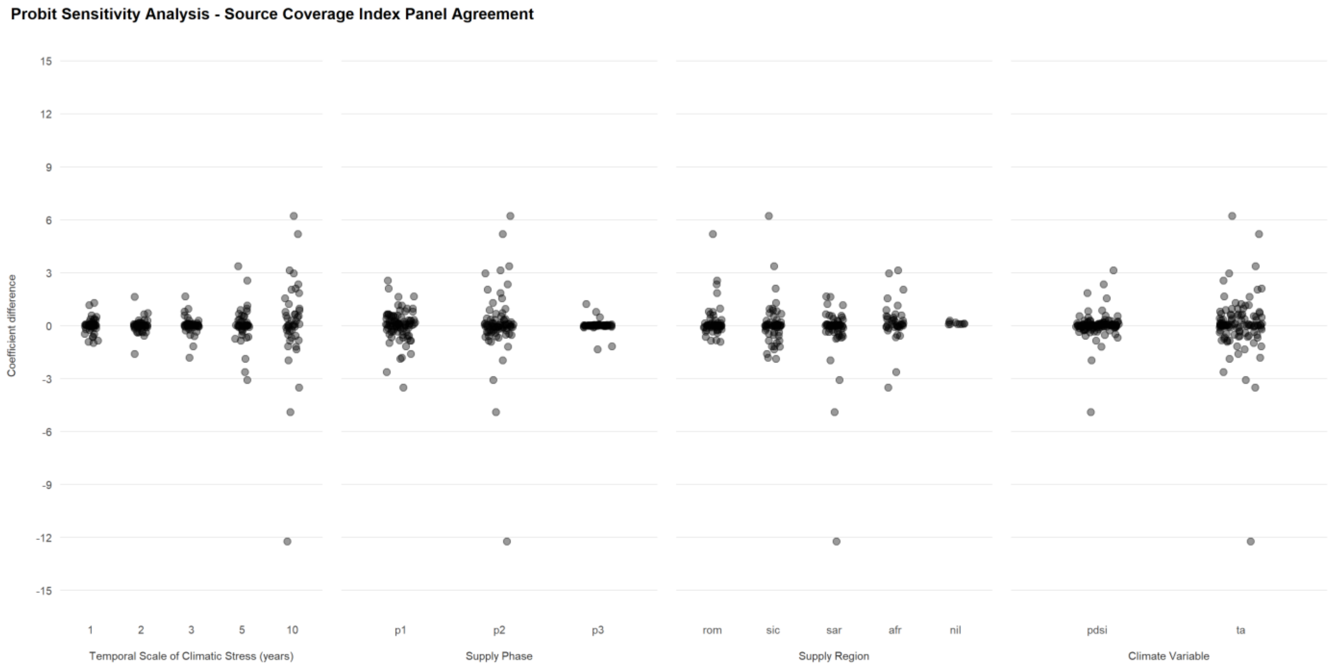

Figure C2. Distribution of the differences in probit regression coefficients between the main model and the model including the historical source coverage index. Points are grouped by temporal averaging window, supply phase, supply region, and climatic variable.

Monte Carlo Approach

For the Monte Carlo analysis, the complete simulation workflow was repeated using the source-coverage-filtered dataset including only years falling within periods of moderate-to-high independent source coverage (coverage index ≥ 2; Table 2 in the main text), thereby restricting both the observed event chronology and the randomisation procedure to the same subset of years. In both the original and filtered analyses, the same supply phases, supply regions, temporal aggregation windows, climatic variables, and simulation settings were used, with only the underlying event chronology modified by the source-coverage filter. This approach reduces the likelihood that the analysis is influenced by false negatives, that is, years in which genuine food shortages occurred but remain unattested because of documentary coverage. To assess robustness, the observed kernel density estimates were evaluated point-by-point against the corresponding Monte Carlo simulation envelope, with each point classified as lying below, above, or within the envelope. Agreement was then quantified by comparing these classifications between the original and source-coverage-filtered analyses. Overall agreement is the percentage of all pointwise comparisons for which the original and source-coverage-filtered analyses produced the same confidence envelope classification. Agreement was also calculated separately for each combination of supply phase, supply region, and temporal aggregation window (hereafter referred to as a panel). Panel agreement was summarised using the median, interquartile range (IQR), and range (Table C2). Panel-specific agreement values and summary statistics for all 115 panels are presented in Figures C3 and C4, respectively.

https://doi.org/10.5194/egusphere-2026-4354
Preprint. Discussion started: 28 July 2026

The Monte Carlo classifications are generally consistent between the original and source-coverage-filtered analyses. Overall agreement is 87.3%, indicating that both analyses assign the same confidence envelope classification in most pointwise comparisons. Agreement is likewise high at the panel level, with a median agreement of 89.6% (IQR: 81.3–95.2%), although panel-specific agreement ranges from 56.2% to 100% (Table C2). Panel-specific results (Figs. C3 and C4) show that lower agreement is observed only in a relatively small number of sensitivity-analysis panels, whereas most panels exhibit high levels of agreement, with complete agreement observed for several panel combinations. Lower levels of agreement are confined to a relatively small number of panels and are most pronounced for scPDSI, which displays greater variability in agreement than the TA reconstructions. No consistent pattern of lower agreement is evident across temporal aggregation windows, supply phases, or supply regions.

Table C2. Summary statistics of the agreement between Monte Carlo simulation envelopes and the original model across the 55 sensitivity analysis panels (combinations of supply phase, supply region, climatic variable and temporal aggregation window.

Statistic	Original vs Historical Source Coverage
Number of panel pairs compared	115
Number of pointwise pairs compared	1,117,760 (1,024 per panel)
Overall agreement (%)	87.3
Median panel agreement (%)	89.6
IQR panel agreement (%)	81.4–95.3
Range panel agreement (%)	56.2–100

https://doi.org/10.5194/egusphere-2026-4354
Preprint. Discussion started: 28 July 2026

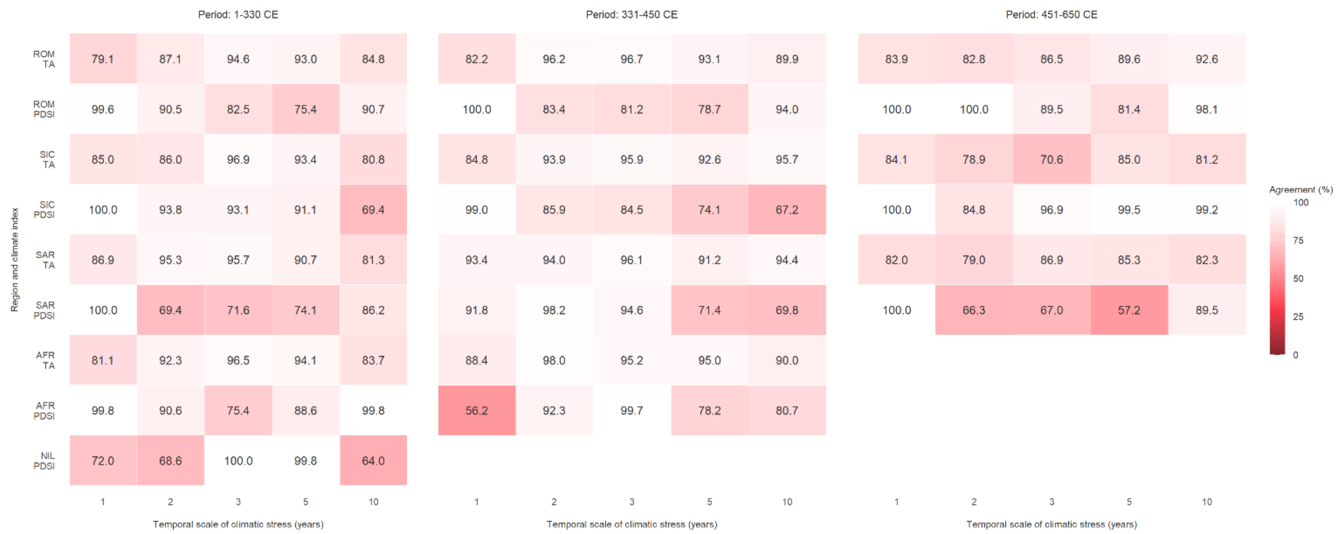

Figure C3. Heatmaps showing the percentage agreement in Monte Carlo confidence envelope classification between the main model and the model including the historical source coverage index. Rows represent regions and climatic indices (TA = temperature anomaly; PDSI = scPDSI). Columns show temporal averaging windows (1–10 years).

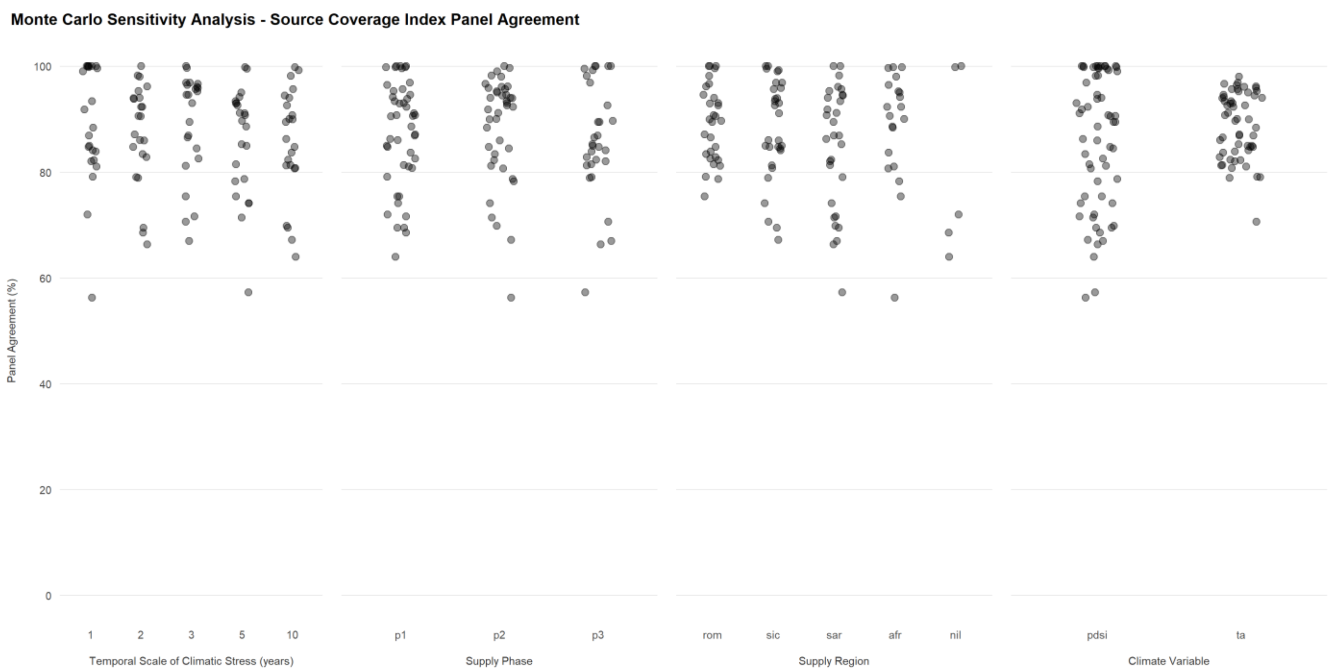

Figure C4. Distribution of Monte Carlo panel-level agreement between the original models and those that include the historical source coverage index. Points are grouped by temporal averaging window, supply phase, supply region, and climatic variable.

Data availability

The Paleo Hydrodynamics Data Assimilation (PHYDA) and Great Eurasian Drought Atlas (GEDA) are publicly available through https://zenodo.org/records/1198817 and http://drought.memphis.edu/GEDA/, respectively. The food shortage database for ancient Rome and the processed palaeoclimatic datasets used to generate the analyses and figures will be made publicly available upon acceptance of the manuscript either through a public data repository or as supplementary material.

Supplement link

The link to the supplement will be included by Copernicus, if applicable.

Author contributions

DT: conceptualisation, data curation, formal analysis, methodology, visualisation, writing (original draft), writing (review & editing). LO: conceptualisation, formal analysis, methodology, writing (review and editing). DKJ: conceptualisation, data curation, writing (review and editing). DVK: conceptualisation, writing (review and editing). PE: conceptualisation, data curation, funding acquisition, writing (review and editing).

Competing interests

The authors declare that they have no conflict of interest.

Disclaimer

Publisher's note: Copernicus Publications remains neutral with regard to jurisdictional claims made in the text, published maps, institutional affiliations, or any other geographical representation in this paper. While Copernicus Publications makes every effort to include appropriate place names, the final responsibility lies with the authors. Views expressed in the text are those of the authors and do not necessarily reflect the views of the publisher.

Financial support

This work is part of the project '*Zooming in on climate and societal change in Central Italy, Late Republic to Late Antiquity*', funded by the Research Foundation – Flanders (FWO) through a senior research project in fundamental research (grant no. G005221N) and was carried out at the Vrije Universiteit Brussel (Belgium) within the Research Group Transdisciplinary Agrifood Studies (TAFS). Part of the work was also conducted during fellowships awarded by the

https://doi.org/10.5194/egusphere-2026-4354
Preprint. Discussion started: 28 July 2026

Structural Determinants of the Roman Economy (SDEP) Research Network to Duncan Keenan-Jones, and the Brussels Institute for Advanced Study (BRIAS) to Devi Taelman.

References

Amrhein, D. E., Hakim, G. J., and Parsons, L. A.: Quantifying Structural Uncertainty in Paleoclimate Data Assimilation with an Application to the Last Millennium, Geophysical Research Letters, 47, e2020GL090485, https://doi.org/10.1029/2020GL090485, 2020.

Anchukaitis, K. J. and Smerdon, J. E.: Progress and uncertainties in global and hemispheric temperature reconstructions of the Common Era, Quaternary Science Reviews, 286, 107537, https://doi.org/10.1016/j.quascirev.2022.107537, 2022.

Bernard, S., McConnell, J., Di Rita, F., Michelangeli, F., Magri, D., Sadori, L., Masi, A., Zanchetta, G., Bini, M., Celant, A., Trentacoste, A., Lodwick, L., Samuels, J. T., Lippi, M. M., Bellini, C., Paparella, C., Peralta, D. P., Tan, J., Van Dommelen, P., De Giorgi, A. U., and Cheung, C.: An Environmental and Climate History of the Roman Expansion in Italy, The Journal of Interdisciplinary History, 54, 1–41, https://doi.org/10.1162/jinh_a_01971, 2023.

Canter, H. V.: Conflagrations in Ancient Rome, The Classical Journal, 27, 270–288, 1932.

Cook, B. I., Cook, E. R., Anchukaitis, K. J., and Singh, D.: Characterizing the 2010 Russian heatwave-Pakistan flood concurrent extreme over the last millennium using the Great Eurasian Drought Atlas, Journal of Climate, 37, 4389–4401, https://doi.org/10.1175/JCLI-D-23-0773.1, 2024.

Daems, D., Cleymans, S., and Vandam, R.: Deep-time patterns of sustainability and resilience in socio-ecological systems: An Introduction to the Special Issue, The Holocene, 34, 1419–1421, https://doi.org/10.1177/09596836241259787, 2024.

Degroot, D.: Climate change and society in the 15th to 18th centuries, WIREs Climate Change, 9, e518, https://doi.org/10.1002/wcc.518, 2018.

Degroot, D., Anchukaitis, K., Bauch, M., Burnham, J., Carnegy, F., Cui, J., de Luna, K., Guzowski, P., Hambrecht, G., Huhtamaa, H., Izdebski, A., Kleemann, K., Moesswilde, E., Neupane, N., Newfield, T. P., Pei, Q., Xoplaki, E., and Zappia, N.: Towards a rigorous understanding of societal responses to climate change, Nature, 591, 539–550, https://doi.org/10.1038/s41586-021-03190-2, 2021.

Degroot, D., Anchukaitis, K. J., Tierney, J. E., Riede, F., Manica, A., Moesswilde, E., and Gauthier, N.: The history of climate and society: a review of the influence of climate change on the human past, Environ. Res. Lett., 17, 103001, https://doi.org/10.1088/1748-9326/ac8faa, 2022.

Deij, E. W. M., Harper, K., Heuvelink, E., and De Beurs, K. M.: Simulating agricultural fragility in past societies: climate change, wheat, and grapes in ancient Rome, Climatic Change, 179, 102, https://doi.org/10.1007/s10584-026-04195-4, 2026.

Eldardiry, H. and Hossain, F.: Understanding Reservoir Operating Rules in the Transboundary Nile River Basin Using Macroscale Hydrologic Modeling with Satellite Measurements, Journal of Hydrometeorology, 20, 2253–2269, https://doi.org/10.1175/JHM-D-19-0058.1, 2019.

Erdkamp, P.: Feeding Rome or feeding Mars? A long-term approach to C. Gracchus' lex frumentaria, Ancient Society, 30, 53–70, 2000.

Erdkamp, P.: The Grain Market in the Roman Empire. A Social, Political and Economic Study, Cambridge University Press, Cambridge, 2005.

Erdkamp, P.: The food supply of the capital, in: The Cambridge Companion to Ancient Rome, edited by: Erdkamp, P., Cambridge University Press, 262–277, https://doi.org/10.1017/CCO9781139025973.019, 2013.

Erdkamp, P.: Famine and Hunger in the Roman World, in: The Routledge Handbook of Diet and Nutrition in the Roman World, edited by: Erdkamp, P. and Holleran, C., Routledge, London, 296–307, 2019.

Erdkamp, P.: A Historian's Introduction to Paleoclimatology, in: Climate Change and Ancient Societies in Europe and the Near East, edited by: Erdkamp, P., Manning, J. G., and Verboven, K., Springer International Publishing, Cham, 1–24, https://doi.org/10.1007/978-3-030-81103-7_1, 2021.

Finné, M., Woodbridge, J., Labuhn, I., and Roberts, C. N.: Holocene hydro-climatic variability in the Mediterranean: A synthetic multi-proxy reconstruction, The Holocene, 29, 847–863, https://doi.org/10.1177/0959683619826634, 2019.

Garnsey, P.: Famine and Food Supply in the Graeco-Roman World. Responses to Risk and Crisis, Cambridge University Press, Cambridge, https://doi.org/10.1017/CBO9780511583827, 1988.

Geraci, G.: Feeding Rome: The Grain Supply, in: A Companion to the City of Rome, edited by: Holleran, C. and Claridge, A., Wiley, 219–245, https://doi.org/10.1002/9781118300664.ch10, 2018.

Guidoboni, E., Comastri, A., and Traina, G.: Catalogue of Ancient Earthquakes in the Mediterranean Area up to the 10th Century, Istituto Nazionale di Geofisica, Rome, 1994.

Haldon, J., Elton, H., Huebner, S. R., Izdebski, A., Mordechai, L., and Newfield, T. P.: Plagues, climate change, and the end of an empire: A response to Kyle Harper's The Fate of Rome (1): Climate, History Compass, 16, e12508, https://doi.org/10.1111/hic3.12508, 2018.

Heinrich, F. B. . J. and Hansen, A. M.: A Hard Row to Hoe: Ancient Climate Change from the Crop Perspective, in: Climate Change and Ancient Societies in Europe and the Near East, edited by: Erdkamp, P., Manning, J. G., and Verboven, K., Springer International Publishing, Cham, 25–80, https://doi.org/10.1007/978-3-030-81103-7_2, 2021.

Heinrich, F. B. J.: Modelling Crop-Selection in Roman Italy. The Economics of Agricultural Decision Making in a Globalizing Economy, in: The Economic Integration of Roman Italy, vol. 404, edited by: de Haas, T. and Tol, G., Brill, Leiden, 141–169, https://doi.org/10.1163/9789004345027_008, 2017.

Huebner, S. R.: Navigating the Nile: Environmental Variability and Socio-Economic Resilience in Roman Egypt, in: The Roman Climate Optimum, edited by: Huebner, S. R. and McDonald, B. T., Springer International Publishing, Cham, in press.

Labuhn, I., Finné, M., Izdebski, A., Roberts, C. N., and Woodbridge, J.: Climatic changes and their impacts in the Mediterranean during the first millennium AD, Late Antiq. Archaeol., 12, 65–88, https://doi.org/10.1163/22134522-12340067, 2016.

https://doi.org/10.5194/egusphere-2026-4354
Preprint. Discussion started: 28 July 2026

Linn, J.: The Roman Grain Supply, 442–455, jla, 5, 298–321, https://doi.org/10.1353/jla.2012.0015, 2012.

Marx, W., Haunschild, R., and Bornmann, L.: Climate and the Decline and Fall of the Western Roman Empire: A Bibliometric View on an Interdisciplinary Approach to Answer a Most Classic Historical Question, Climate, 6, 90, https://doi.org/10.3390/cli6040090, 2018.

McCormick, M., Harper, K., More, A. M., and Gibson, K.: Geodatabase of Historical Evidence on Roman and Post-Roman Climate, Harvard Dataverse, https://doi.org/10.7910/DVN/TVXATE, 2012.

Morley, N.: Metropolis and Hinterland: The City of Rome and the Italian Economy, 200 BC–AD 200, 1st ed., Cambridge University Press, https://doi.org/10.1017/CBO9780511518584, 1996.

R Core Team: R: A language and environment for statistical computing, R Foundation for Statistical Computing, Vienna, 2026.

Rickman, G.: The corn supply of ancient Rome, Special ed. for Sandpiper Books Ltd., Clarendon Press, Oxford, 1980.

Slavin, P.: Climate and famines: a historical reassessment, WIREs Climate Change, 7, 433–447, https://doi.org/10.1002/wcc.395, 2016.

Smerdon, J. E., Cook, E. R., and Steiger, N. J.: The Historical Development of Large-Scale Paleoclimate Field Reconstructions Over the Common Era, Reviews of Geophysics, 61, e2022RG000782, https://doi.org/10.1029/2022RG000782, 2023.

Stathakopoulos, D. C.: Famine and Pestilence in the Late Roman and Early Byzantine Empire. A Systematic Survey of Subsistence Crises and Epidemics, Ashgate, Aldershot, 2004.

Steiger, N. J., Smerdon, J. E., Cook, E. R., and Cook, B. I.: A reconstruction of global hydroclimate and dynamical variables over the Common Era, Sci Data, 5, 180086, https://doi.org/10.1038/sdata.2018.86, 2018.

Taelman, D., Erdkamp, P., Keenan-Jones, D., Heinrich, F. B. J., Hansen, A. M., Corona, C., Drysdale, R. N., Stoffel, M., Verdon-Kidd, D. C., and Zanchetta, G.: Climate and Societal Change in Central Italy, from Late Republic to Late Antiquity, in: The Roman Climate Optimum, edited by: Huebner, S. R. and McDonald, B. T., Springer International Publishing, Cham, in press.

Taylor, R.: Bread and Water: Septimius Severus and the Rise of the Curator Aquarum Et Miniciae, Memoirs of the American Academy in Rome, 55, 199–220, 2010.

Tierney, J. E., Judd, E. J., Osman, M. B., King, J. M., Truax, O. J., Steiger, N. J., Amrhein, D. E., and Anchukaitis, K. J.: Advances in Paleoclimate Data Assimilation, Annual Review of Earth and Planetary Sciences, 53, 625–650, https://doi.org/10.1146/annurev-earth-032320-064209, 2025.

Van Bavel, B. J. P., Curtis, D. R., Hannaford, M. J., Moatsos, M., Roosen, J., and Soens, T.: Climate and society in long-term perspective: Opportunities and pitfalls in the use of historical datasets, WIREs Climate Change, 10, e611, https://doi.org/10.1002/wcc.611, 2019.

Watson, R. T., Albritton, D. L., and Intergovernmental Panel on Climate Change (Eds.): Climate change 2001: synthesis report, Cambridge University Press, Cambridge - New York, 397 pp., 2001.

https://doi.org/10.5194/egusphere-2026-4354
Preprint. Discussion started: 28 July 2026

Wells, N., Goddard, S., and Hayes, M. J.: A Self-Calibrating Palmer Drought Severity Index, Journal of Climate, 17, 2335–2351, 2004.

White, S., Pei, Q., Kleemann, K., Dolák, L., Huhtamaa, H., and Camenisch, C.: New perspectives on historical climatology, WIREs Climate Change, 14, https://doi.org/10.1002/wcc.808, 2023.

Wijnendaele, J. W. P.: Late Roman Civil War and the African Grain Supply, Journal of Late Antiquity, 12, 298–328, https://doi.org/10.1353/jla.2019.0018, 2019.

Yitayew, M. and Melesse, A. M.: Critical Water Resources Issues in the Nile River Basin, in: Nile River Basin, edited by: Melesse, A. M., Springer Netherlands, Dordrecht, 401–416, https://doi.org/10.1007/978-94-007-0689-7_20, 2011.